Since January 2020 Elsevier has created a COVID-19 resource centre with free information in English and Mandarin on the novel coronavirus COVID-19. The COVID-19 resource centre is hosted on Elsevier Connect, the company's public news and information website.

Phytomedicine 100 (2022) 154083

Contents lists available at ScienceDirect

Phytomedicine

journal homepage: www.elsevier.com/locate/phymed

Original Article

Gegen Qinlian pills alleviate carrageenan-induced thrombosis in mice model by regulating the HMGB1/NF-κB/NLRP3 signaling

Xiaohan Wei [a,b,c,1], Baoping Zhang [a,b,c,1], Feiyan Wei [a,b,c], Mengze Ding [a,b,c], Zhenye Luo [a,b,c], Xinlong Han [a,b,c], Xiaomei Tan [a,b,c,*]

[a] School of Traditional Chinese Medicine, Southern Medical University, Guangzhou 510515, China
[b] Guangzhou Provincial Key Laboratory of Chinese Medicine Pharmaceutics, Guangzhou 510515, China
[c] Guangdong Provincial Engineering Laboratory of Chinese Medicine Preparation Technology, Guangzhou 510515, China

ARTICLE INFO

Chemical compounds studied in this article:
puerarin (PubChem CID: 5281807)
daidzin (PubChem CID: 107971)
genistin (PubChem CID: 5281377)
baicalin (PubChem CID: 64982)
wogonoside (PubChem CID: 3084961)
berberine (PubChem CID: 2353)
jatrorrhizine (PubChem CID: 72323)
palmatine (PubChem CID: 19009)
liquiritin (PubChem CID: 503737)
and glycyram (PubChem CID: 3495)

Keywords:
COVID-19
Gegen Qinlian Pills
HMGB1/NFκB/NLRP3 signaling
Hyperinflammatory
Thrombosis

ABSTRACT

Background: The high incidence of thrombotic events is one of the clinical characteristics of coronavirus disease of 2019 (COVID-19), due to a hyperinflammatory response caused by the virus. Gegen Qinlian Pills (GQP) is a Traditional Chinese Medicine that is included in the Chinese Pharmacopoeia and played an important role in the clinical fight against COVID-19. Although GQP has shown the potential to treat thrombosis, there is no relevant research on its treatment of thrombosis so far.
Hypothesis: We hypothesized that GQP may be capable inhibit inflammation-induced thrombosis.
Study Design: We tested our hypothesis in a carrageenan-induced thrombosis mouse model *in vivo* and lipopolysaccharide (LPS)-induced human endothelial cells (HUVECs) *in vitro*.
Methods: We used a carrageenan-induced mouse thrombus model to confirm the inhibitory effect of GQP on inflammation-induced thrombus. *In vitro,* studies in human umbilical vein endothelial cells (HUVECs) and *in silico* network pharmacology analyses were performed to reveal the underlying mechanisms of GQP and determine the main components, targets, and pathways of GQP, respectively.
Results: Oral administration of 227.5 mg/kg, 445 mg/kg and 910 mg/kg of GQP significantly inhibited thrombi in the lung, liver, and tail and augmented tail blood flow of carrageenan-induced mice with reduced plasma tumor necrosis factor α (TNF-α) and diminished expression of high mobility group box 1 (HMGB1) in lung tissues. GQP ethanol extract (1, 2, or 5 μg/ml) also reduced the adhesion of platelets to LPS stimulated HUVECs. The TNF-α and the expression of HMGB1, nuclear factor kappa B (NF-κB), and NLR family pyrin domain containing 3 (NLRP3) in LPS stimulated HUVECs were also attenuated. Moreover, we analyzed the components of GQP and inferred the main targets, biological processes, and pathways of GQP in the treatment of inflammation-induced thrombosis through network pharmacology.
Conclusion: Overall, we demonstrated that GQP could reduce inflammation-induced thrombosis by inhibiting HMGB1/NFκB/NLRP3 signaling and provided an accurate explanation for the multi-target, multi-function mechanism of GQP in the treatment of thromboinflammation, and provides a reference for the clinical usage of GQP.

Introduction

The outbreak of severe acute respiratory syndrome coronavirus 2 (SARS-CoV-2) in 2019 poses a major threat to international health and the economy. The high incidence of thrombotic events is one of the clinical characteristics of SARS-CoV-2-related disease, known as

Abbreviations: CFSE, 5,6-Carboxyfluorescein diacetate succinimidyl ester; COVID-19, Coronavirus disease 2019; D-I-T-D, Drug-Ingredients-Targets-Diseases; ELISA, Enzyme-linked immunosorbent assay; GO, Gene ontology; GQP, Gegen Qinlian pill; GQP-EE, GQP ethanol extract; HE, Hematoxylin and eosin; HPLC, High-performance liquid chromatography; HUVEC, Human umbilical vein endothelial cell; KEGG, Kyoto Encyclopedia of Genes and Genomes; LPS, Lipopolysaccharides; PBS, Physiological saline; PE, Pulmonary embolism; PPI, Protein-protein interaction; SARS-CoV-2, Severe acute respiratory syndrome coronavirus 2.

* Corresponding author.
E-mail address: tanxm_smu@163.com (X. Tan).
[1] The authors contributed equally to the work.

https://doi.org/10.1016/j.phymed.2022.154083
Received 4 November 2021; Received in revised form 19 March 2022; Accepted 26 March 2022
Available online 1 April 2022

coronavirus disease 2019 or COVID-19 (Katneni et al., 2020). In patients with COVID-19, hypercoagulability and hyperinflammation are accompanied by higher morbidity and mortality rates (Rad et al., 2021). The rate of radiographically confirmed venous thromboembolism in COVID-19 patients was reported to be 4.8% (Al-Samkari et al., 2020). Moreover, In severe patients, the cumulative incidence of symptomatic acute pulmonary embolism (PE), deep vein thrombosis (DVT), and other thrombotic complications can reach up to 31%, with PE as the most frequent thrombotic complication (Klok et al., 2020). Hyper-inflammation plays an important role in the development of thrombotic complications in COVID-19 (Biswas and Khan, 2020). Indeed, the inflammatory response can block fibrinolysis, and activate endothelial cells and innate immune cells by releasing several factors (such as the von Willebrand Factor, tissue factor, and neutrophil extracellular traps), thus promoting thrombosis (Engelmann and Massberg, 2013). -

Gegen Qinlian pills (GQP) are a Traditional Chinese Medicine (TCM) that is included in the Chinese Pharmacopoeia, to treat acute infectious diarrhea, infantile autumn diarrhea, and fever and headache caused by colds. It consists of four herbs: *Pueraria montana* var. lobata (Willd.) Sanjappa & Pradeep (Gegen), *Scutellaria baicalensis* Georgi (Huangqin), *Coptis chinensis* Franch. (Huanglian) and G*lycyrrhiza uralensis* Fisch. (Gancao). A clinical study on GQP for the treatment of COVID-19 showed that it can prevent the development of severe disease, significantly ameliorating the symptoms of cough, chest tightness, nausea, and vomiting, as well as by significantly shorting the time of nucleic acid conversion, and prevent lung inflammation (Linqun et al., 2020). It has been reported that GQP can down-regulate inflammatory cytokines and alleviate colitis inflammation by suppressing toll-like receptor 4 (TLR4)/nuclear factor kappa B (NF-κB) signaling (Li et al., 2016). Moreover, the active compounds of GQP (puerarin, daidzin, and berberine) have been shown to have an antithrombotic effect (Choo et al., 2002; Zhang et al., 2016). Thus, we hypothesized that GQP may prevent and treat inflammation-induced thrombosis by regulating the inflammatory response.

Endothelial cells play an important role in maintaining vascular homeostasis and regulating the coagulation system (Watanabe-Kusunoki et al., 2020). In inflammation disorders, various proinflammatory factors lead to vascular inflammation and epithelial cell dysfunction, increases expression of vascular cell adhesion molecule 1 (VCAM-1), intercellular adhesion molecule 1 (ICAM-1), and von Willebrand factor (vWF), further leading to platelets adhesion and thrombosis (Katneni et al., 2020).

High mobility group box 1 (HMGB1) is a well-known damage-associated molecular pattern (DAMP) molecule, generally located in the cell nucleus. Under pathological conditions, it can be released from immune or dying cells, and activate the innate immune system, triggering vascular injury (Kim and Lee, 2020). It is overexpressed in patients with thrombi and pharmacologic inhibition of HMGB1 prevents the formation of DVT (Stark et al., 2016; Xu et al., 2018). Moreover, HMGB1 is closely related to the NF-κB signaling and triggers the activation of NLR family pyrin domain containing 3 (NLRP3) inflammasome in an NF-κB-dependent manner. NLRP3 inflammasome is a cytosolic signaling complex that actives caspase 1 and triggers the release of interleukin-1β (IL-1β) aggravate the inflammatory response and lead to cell death (Mangan et al., 2018). Thus, the agents inhibiting HMGB1 expression may have great potential in treating inflammation-induced thrombosis.

In this study, we aimed to confirm the inhibitory effect of GQP on a carrageenan-induced thrombus mouse model. Additional *in vitro* studies in human umbilical vein endothelial cells (HUVECs) and *in silico* network pharmacology analyses were performed to shed light into the underlying mechanisms of GQP and determine the main components, targets, and pathways of GQP, respectively.

Materials and methods

Reagents

Aspirin Tablets were purchased from Bayer S.p.A (Viale Certosa, Milano, Italy). Adenosine diphosphate (ADP) was purchased from TargetMol (Wellesley Hills, MA, USA). BoxA was purchased from HMGBiotech (Via Olgettina, Milano, Italy). Carrageenan was purchased from Sigma-Aldrich (St Louis, MO, USA). ECL was purchased from Affinity Biosciences (OH, USA). GQP was purchased from Huahong Pharmaceutical Co. Ltd (BatchNo. 20191002; Liuzhou, China). CFSE and PGE1 were purchased from Cayman Chemical (Ann Arbor, MI, USA). N4-Acetylcytidine triphosphate sodium was purchased from Good Laboratory Practice Bioscience (Montclair, California, USA). Thrombin was provided from Macklin Biochemical (Shanghai, China).

Rabbit anti-HMGB1 (Cat# 6893S), IκBα (Cat# 4060L), NF-κBp65 (Cat# 8242T), p-NF-κBp65 (Cat# 3033T), NLRP3 (Cat# 15101S) and HRP-linked Antibody (Cat# 7074S) were purchased from Cell Signaling Technology (Danvers, MA, USA). β-actin (Cat# AF7018), Caspase 1 (Cat# AF5418) and p-IκBα (Cat# AF2002) were purchased from Affinity Biosciences.

Animals

BALB/c mice (male, 18-22 g) were purchased from the Model Animal Research Centre of Southern Medical University (Guangzhou, China) and maintained under specific pathogen-free (SPF) conditions. The protocol of animal experiments was approved and conducted according to the guidelines of the Animal Ethics Committee of Southern Medical University (Resolution No. SMUL2020135; Date of Resolution 2020.10.10).

Dose and treatment

Random allocation was performed to divide fifty-four mice into nine groups (six mice in each group): naïve, model, GQP treatment low dose (treatment-L; 227.5 mg/kg), GQP treatment median dose (treatment-M; 445 mg/kg), GQP treatment high dose (treatment-H; 910 mg/kg), GQP prevention low dose (prevention-L; 227.5 mg/kg), GQP prevention median dose (prevention-M; 445 mg/kg), GQP prevention high dose (prevention-H; 910 mg/kg), and aspirin (22.75 mg/kg) groups. The naïve and model groups received physiological saline (PBS) intragastrically for 9 d; the treatment groups received PBS for 7 d, followed by GQP suspension (227.5, 445, or 910 mg/kg) for 2 d; the prevention groups received GQP suspension at the same doses for 9 d, and the aspirin group was administered aspirin (22.75 mg/kg) for 9 d. Seven days after administration, except for the control group, all the other groups were injected intraperitoneally with 10 μl/g of carrageenan solution at a dose of 100 mg/kg body weight (Li et al., 2019). Two days later, all mice were anesthetized with 1% pentobarbital sodium and mouse tails were photographed and immediately assessed for blood flow. Then blood, tail, liver, and lung samples were collected (Fig. 1).

Blood flow monitoring

After anesthetized, the mice were placed on the absorption mat with the surface of their tails perpendicular to the laser beam. Blood flow was recorded by RWD RFLSI Pro+ Laser Speckle Contrast Imaging (Shenzhen, China) and continuously monitored 5 min after anesthetization. The LSCI instrument brought out the blood perfusion signals in the form of number (volts, V) and color-coded images. The low perfusion was displayed dark blue and high perfusion was showed bright red.

Blood cells counting

Blood samples were collected from mice into clean tubes containing

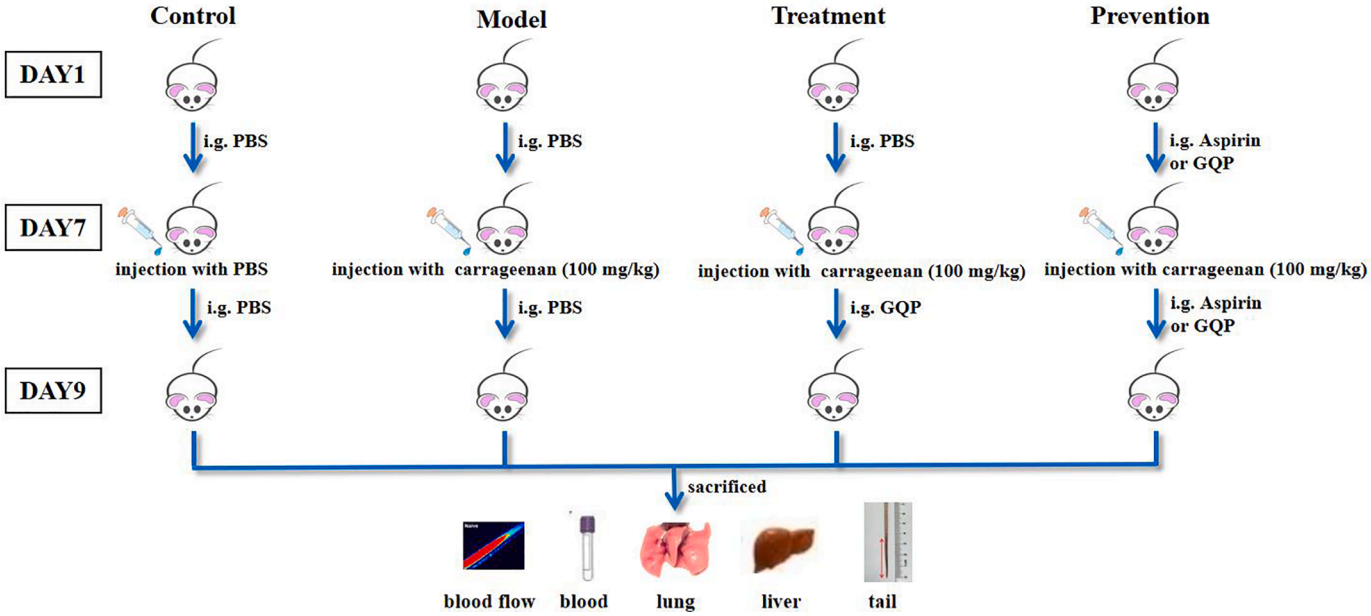

Fig. 1. Schematic diagram of the *in vivo* experiments. The naïve and model groups received PBS intragastrically for 9 d; the treatment groups received GQP suspension (227.5, 445, or 910 mg/kg) for the last 2 d of the experimental period. Prevention groups received GQP suspension at the same doses for 9 d, whereas the aspirin group was administered aspirin (22.75 mg/kg) for 9 d. Except for the control group, all the other groups were injected with carrageenan solution (100 mg/kg) on day 7. On day 9, all mice were euthanized, and mouse tails were photographed and evaluated for blood flow. Blood, tail, liver, and lung samples were collected for further analyses.

2.7% ethylenediaminetetraacetic acid dipotassium salt solution and examined by Sysmex XN 1000 automatic blood cell analyzer (Sysmex, Kobe, Japan).

Hematoxylin and eosin (HE) staining and Immunohistochemical (IHC) staining

To determine the formation of thrombus in mice tissue, mouse tail at 2, 4, 6 cm distance from the tip of the tail, as well as liver or lung specimens were placed in 4% paraformaldehyde overnight, incubated in 30% sucrose solution overnight, and then embedded in paraffin solution. Paraffin sections (5 μm) were prepared for HE staining. Moreover, the 5-μm paraffin sections of the lung were subjected to immunohistochemical assay using the primary antibody (HMGB1 (1:100), NLRP3 (1:100), p-NF-κBp65 (1:100) or p-IκBα (1:50)) and DAB substrate kit was used to specific labeling with these proteins respectively. The images of HE and IHC were obtained using a DMi8 microscope (Leica Microsystems, Wetzlar, Germany).

Cell culture

Human umbilical vein endothelial cells (HUVECs) were supplied by Jennio (Guangzhou, China), cultured in complete Dulbecco's modified Eagle's medium (Gibco, NY, USA) containing 10% fetal bovine serum (Gibco), 1% Penicillin Streptomycin (Gibco), and maintained at 37 °C under 5% CO_2. Experiments were performed using 8-20 generations of cells.

Preparation of GQP ethanol extract solution

GQP ethanol extract was prepared by the heating reflux extraction method. Briefly, 14 g of GQP was added to 200 ml of ethanol and boiled for 4 h. Afterward, the extract solution was filtered through a brucer funnel while it was hot. After that, the filtrate evaporated in a water bath at 95 °C. The concentrated extract was named GQP ethanol extract (GQP-EE). After GQP-EE was dissolved in PBS, the solution was named GQP ethanol extract solution (GQP-EES) and used for *in vitro* experiments.

Cell viability

HUVECs were placed in 96-well plates at a density of 5×10^3 cells *per* well and then treated with lipopolysaccharides (LPS; 5, 10, 20, 40, or 80 μg/ml), GQP-EES (1, 2, 4, 8, 16, or 32 μg/ml), 5 μg/ml LPS in the presence or absence of GQP-EES (1, 2, or 5 μg/ml), aspirin (10 μg/ml) with 5 μg/ml LPS, or BoxA (10 μg/ml) with 5 μg/ml LPS or N4-Acetylcytidine (N4A) triphosphate sodium (1 mM) with 5 μg/ml LPS for 24 h. Cells were treated by the Cell Counting Kit-8 (CCK-8, Gibco) and measured their option density at 450nm using Synergy Microplate Reader (BioTek, Winooski, VT, USA).

Platelet isolation and labeling

Sprague–Dawley (SD) rats were supplied by the Model Animal Research Centre of Southern Medical University. The rats were anesthetized with 1% pentobarbital sodium, and then blood was collected from the abdominal aorta into clean tubes containing 3.2% sodium citrate solution. After keeping for 30 min at 25 °C, the blood was then centrifuged at 200 × g for 10 min at 25 °C. Platelet-rich plasma was initially added to prostaglandin E1 (1 μM) for 10 min, centrifuged for 10 min at 600 × g at 25 °C, and then washed with PBS. The platelet pellet was resuspended in buffer A (130 mM NaCl, 10 mM sodium citrate, 9 mM $NaHCO_3$, 6 mM dextrose, 0.9 mM $MgCl_2$, 0.81 mM KH_2PO_4, 10 mM Tris, pH 7.4), and warmed to 37 °C before use.

Platelet Aggregation Assay

The platelet was resuspended in buffer A, dispensed into 96-well plates at a concentration of 10^6 cells/ml, and then incubated for 10min at 37 °C in presence of 50 μl of drugs. After that, ADP (25 μM), thrombin (0.5 U/ml), and $CaCl_2$ (1.8 mM) were added just before the assay. The plate was continuously shaken in kinetic mode at 37°C and taken the optical density readings at 405 nm every 1 min for an hour simultaneously.

Adhesion assay

The platelet was labeled with CFSE (1 μM) for 30 min at 37 °C, and then washed to remove free CFSE.

HUVECs were placed in 24-well plates at a density of 5×10^4 cells *per* well and treated with LPS (5 μg/ml), LPS (5 μg/ml) plus GQP-EES (1, 2, or 5 μg/ml), LPS (5 μg/ml) plus aspirin (10 μg/ml), or LPS (5 μg/ml) plus BoxA (10 μg/ml), or LPS (5 μg/ml) plus N4A (1 mM) for 24 h. After treatment, HUVECs were incubated with CFSE-labeled platelets (1×10^5/well) for 30 min at 37 °C and then washed with PBS three times. The platelet adhesion was observed using a Leica DMi8 microscope.

Enzyme-linked immunosorbent assay (ELISA)

Plasma was collected from the top layer of mice blood and used to determine Tumor necrosis factor α (TNF-α) using the TNF-α ELISA kit (Dakewei Biotech, Shenzhen, China).

Cell culture medium was collected from different administration cell groups as described above. The cell culture media were determined Tumor necrosis factor α (TNF-α) and interleukin-1β (IL-1β) using ELISA kits (Dakewei Biotech, Shenzhen, China).

Immunofluorescent (IF) staining

HUVEC was placed in 6-well plates containing slices at a density of 1.5×10^5 cells per well and treated with LPS (5 μg/ml), LPS (5 μg/ml) plus GQP-EES (1, 2, 5 μg/ml) for 24 h. After treatment, the cells were immersed in 4% paraformaldehyde, and blocked with 5% Bull Serum Albumin (Solarbio, Beijing, China), followed by incubation overnight at 4 °C with primary antibody (HMGB1 (1:100), NLRP3 (1:100), p-NF-κBp65 (1:800) or p-IκBα (1:100)) and later incubated with goat anti-rabbit FITC-linked antibody then sealed by Antifade Mounting Medium containing DAPI (Beyotime, Shanghai, China) and were photographed by Zeiss LSM 800 Confocal Laser Scanning Microscopy (Zeiss, Oberkochen, Germany).

Real-time polymerase chain reaction (RT-PCR) analysis

Total RNA was extracted from HUVECs by RNA extraction solution and then purified by trichloromethane, isopropyl alcohol, and anhydrous ethanol in sequence. cDNA was synthesized by First Strand cDNA Synthesis Kit (Servicebio, Wuhan, China), and 2 × SYBR Green qPCR Master Mix (Servicebio) was used for qRT-PCR. Primers (5'-3') were as follows: GAPDH-S, GGAAGCTTGTCATCAATGGAAATC; GAPDH-A, TGATGACC CTTTTGGCTCCC; VCAM1-S, GATAGTCCACTGAATGGGAAGGT; VCAM1-A, AACACTTGACTGTGATCGGCTTC; ICAM1-S, CAGACTCCAATGTGCCA GGC; ICAM1-A, TCTTCCGCTGGCGGTTATA; vWF-S, AATGACCTCAC-CAGCAGCAAC; vWF-A, TCACTGGTAAGGATTCTACAGGAGG.

Western blotting analysis

Total proteins were extracted from lung tissues or HUVECs. The proteins were separated by 10% sodium dodecyl sulfate-polyacrylamide gel electrophoresis and transferred onto polyvinylidene fluoride membranes (0.45 μm) (Merck Millipore, Darmstadt, Germany). Membranes were incubated overnight at 4°C with the primary antibody (HMGB1 (1:1000), Caspase1 (1:1000), NF-κBp65 (1:1000), p-NF-κBp65 (1:1000), NLRP3 (1:1000), IκBα (1:1000), p-IκBα (1:1000), and β-actin 1:5000)) at 4°C overnight, and later 1 h with an HRP-linked secondary antibody. Proteins bands were visualized using ECL substrate and Tanon 5200s Chemiluminescence Imaging system (Tanon, Shanghai, China). Signal plots were processed using Image J 1.8.0 software.

Characterization of GQP compounds by high-performance liquid chromatography (HPLC)

GQP-EE was extracted using ultrasonic methanol. Briefly, GQP powder was mixed with 10 times the amount of methanol and kept ultrasonically for 30 min, diluted to 10 mg/ml with methanol, then filtered through a 0.22-μm membrane. Mixed standard references containing puerarin (5 μg/ml, PubChem CID: 5281807), daidzin (10 μg/ml, PubChem CID: 107971), genistin (2.5 μg/ml, PubChem CID: 5281377), baicalin (10 μg/ml, PubChem CID: 64982), wogonoside (12.5 μg/ml, PubChem CID: 3084961), berberine (10 μg/ml, PubChem CID: 2353), jatrorrhizine (10 μg/ml, PubChem CID: 72323), palmatine (10 μg/m, PubChem CID: 19009), liquiritin (10 μg/ml, PubChem CID: 503737), and glycyram (60 μg/ml, PubChem CID: 3495) were dissolved in ethanol.

Liquid chromatography was performed on Agilent 1260 HPLC system (Agilent Technologies, Santa Clara, CA, USA). A Kromasil 100-5-C18 column (4.6 × 250 mm, 5 μm) was used for the separations at 25°C. The mobile phase system consisted of water containing 0.01% phosphoric acid (A) and acetonitrile (B). The HPLC elution profile was: 0-60 min, 8-30% B; 60-80 min, 30-50% B; 80-85 min, 50-100% B. The flow rate was 1 ml/min, and the monitoring UV wavelength was set at 275 nm with an injection volume of 10 μl.

Network pharmacology analysis

Target Prediction

The corresponding targets of the identified compounds were obtained from the Traditional Chinese Medicine Systems Pharmacology (http://lsp.nwu.edu. cn/tcmsp.php) and Swiss Target Prediction (http://www.swisstargetprediction.ch/). Then we searched the keywords "pulmonary embolism" and "pneumonia" on DisGeNET (http://www.disgenet.org/) and GeneCards (https://www.genecards.org/) databases respectively to collect the gene targets of pulmonary embolism and pneumonia. All the targets obtained were standardized by the UniProt knowledge database. Then we built a Drug-Ingredients-Targets-Diseases (D-I-T-D) network based on interactions between GQP, ingredients, gene targets, and diseases. Finally, we used Cytoscape (Version 3.7.0) to visualize the D-I-T-D network.

Construction of a Protein-Protein Interaction (PPI) Network

To explain the interaction between target proteins, we intersected the obtained drug targets with the genes related to pulmonary embolism and pneumonia and obtained overlapping targets. Then we uploaded the gene symbols of overlapping targets to STRING (http://string-db.org) online website to obtain the PPI data. The organism was limited to "Homo sapiens". To ensure the reliability of this analysis, we constructed the PPI network with a high confidence score of 0.7. The PPI network was analyzed and visualized using Cytoscape.

Gene ontology (GO) function and Kyoto Encyclopedia of Genes and Genomes (KEGG) pathway enrichment analyses

Proteins play biological functions through a variety of interactions and associations, The gene functions and signal pathways related to GQP in the treatment of pulmonary embolism and pneumonia were analyzed by R 3.6.1 software with the Bioconductor package. The *p*-value cutoff was set as 0.05 and the q-value Cutoff as 0.05.

Statistical analyses

Data analysis was performed using Prism 7 (GraphPad Software, San Diego, CA, USA). Differences between groups were assessed by one-way analysis of variance, followed by Tukey's test. A p-value < 0.05 was considered statistically significant. All experiments were repeated three times.

Results

Effects of GQP on the thrombosis rate and tail blood flow in thrombosis mice model

To assess the effects of GQP on the thrombosis mice model, we determined the thrombosis rate (thrombosis length/the whole tail length) in the different treatment groups. As shown in Fig. 2A, C, both GQP treatment groups and prevention groups showed significantly ($p < 0.01$) reduced tail thrombosis rate compared with the model group. The effect of the middle dose group was better than that of the low dose group and high dose group, but no statistically significant differences were observed among the GQP doses. In addition, no significant difference ($p > 0.05$) between the aspirin and model groups was noted.

The blood flow of 1.5 cm from the tip of the tail was detected via Laser Speckle Flowgraphy. Overall, the blood flow of the model group was significantly ($p < 0.01$) decreased compared with the naïve group, and GQP could reverse this situation (Fig. 2B, D). Aspirin also increased the blood flow, but there was no significant difference ($p > 0.05$) between the aspirin and model groups. These results indicate that GQP is more effective than aspirin in reducing carrageenan-induced thrombus formation in mice.

Effects of GQP on tissue thrombosis induced by carrageenan in mice

48 h after intraperitoneal injection of carrageenan, the mice were euthanized and their tail, liver, and lung tissues were collected for general morphology analysis. The tail vessels (blue dotted lines) at 2 and 4 cm positions of the mice in the model group were almost fully occupied by a thrombus (red dotted lines), while nearly 60% of the vessels at the 6 cm position were occupied by thrombi (Fig. 3A). Both GQP treatment and prevention groups inhibited the formation of thrombosis, with little thrombosis being detected at the 6 cm position. The thrombus at 6 cm position in the aspirin group was also decreased to about 20%.

There were venous thrombosis (black arrows), extensive capillary hemorrhage, and inflammatory infiltration in the lung tissue of the model group compared with the naive group. In the aspirin group, thrombus and inflammatory infiltration were still observed. However, thrombosis in pulmonary vessels was inhibited by GQP, and inflammatory infiltration was also reduced in GQP groups (Fig. 3B, D).

In liver tissue, hepatic vein thrombosis (blue arrows, Fig. 3C), hepatocyte edema, inflammatory infiltration, and local aggregation around blood vessels (yellow arrows, Fig. 3C) were observed. Similarly, GQP (treatment and prevention groups) inhibited hepatic vein thrombosis and hepatocyte edema significantly regulated inflammatory infiltration (Fig. 3C, E).

Effects of GQP on the peripheral hemogram of carrageenan-induced thrombosis mice

Hematological analysis showed that 48 h after carrageenan was injected intraperitoneally, leukocyte count (WBC), monocyte count (MONON), hemoglobin (HGB), and mean platelet volume (MPV) in the peripheral blood of the model group were significantly ($p < 0.01$) increased compared with the naïve group. There was no significant difference in other indexes between these groups. Aspirin and GQP could downregulate WBC, MONON, and MPV, but had no obvious effect on HGB (Fig. 4A-D).

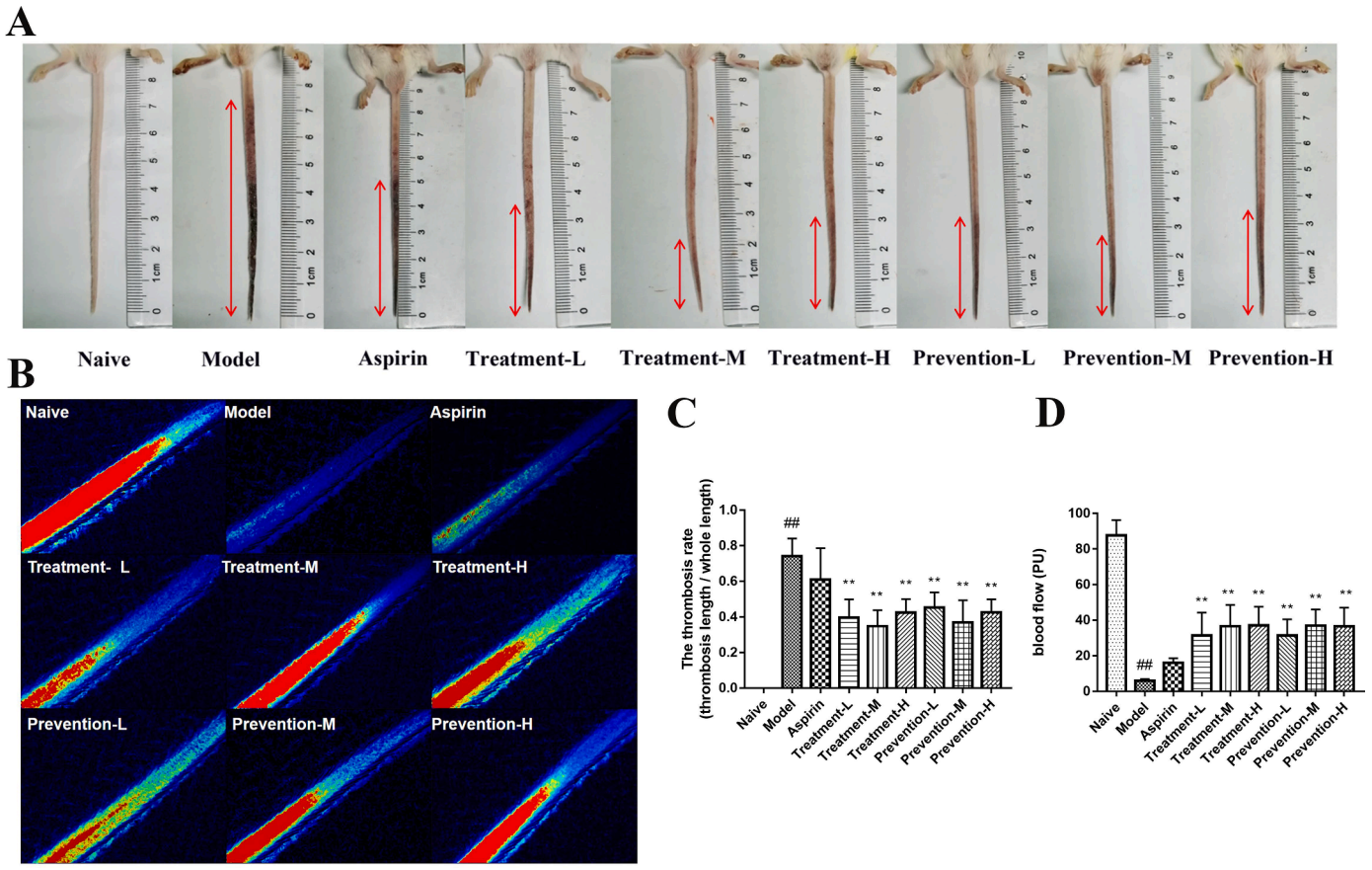

Fig. 2. Effects of Gegen Qinlian pills (GQP) on carrageenan-induced thrombosis in mice. (A) Thrombus length, (B, D) blood flow, and (C) thrombosis rate in the tail of carrageenan-induced thrombosis mice. ## $p < 0.01$ *versus* naïve group, ** $p < 0.01$ *versus* model group (n = 6).

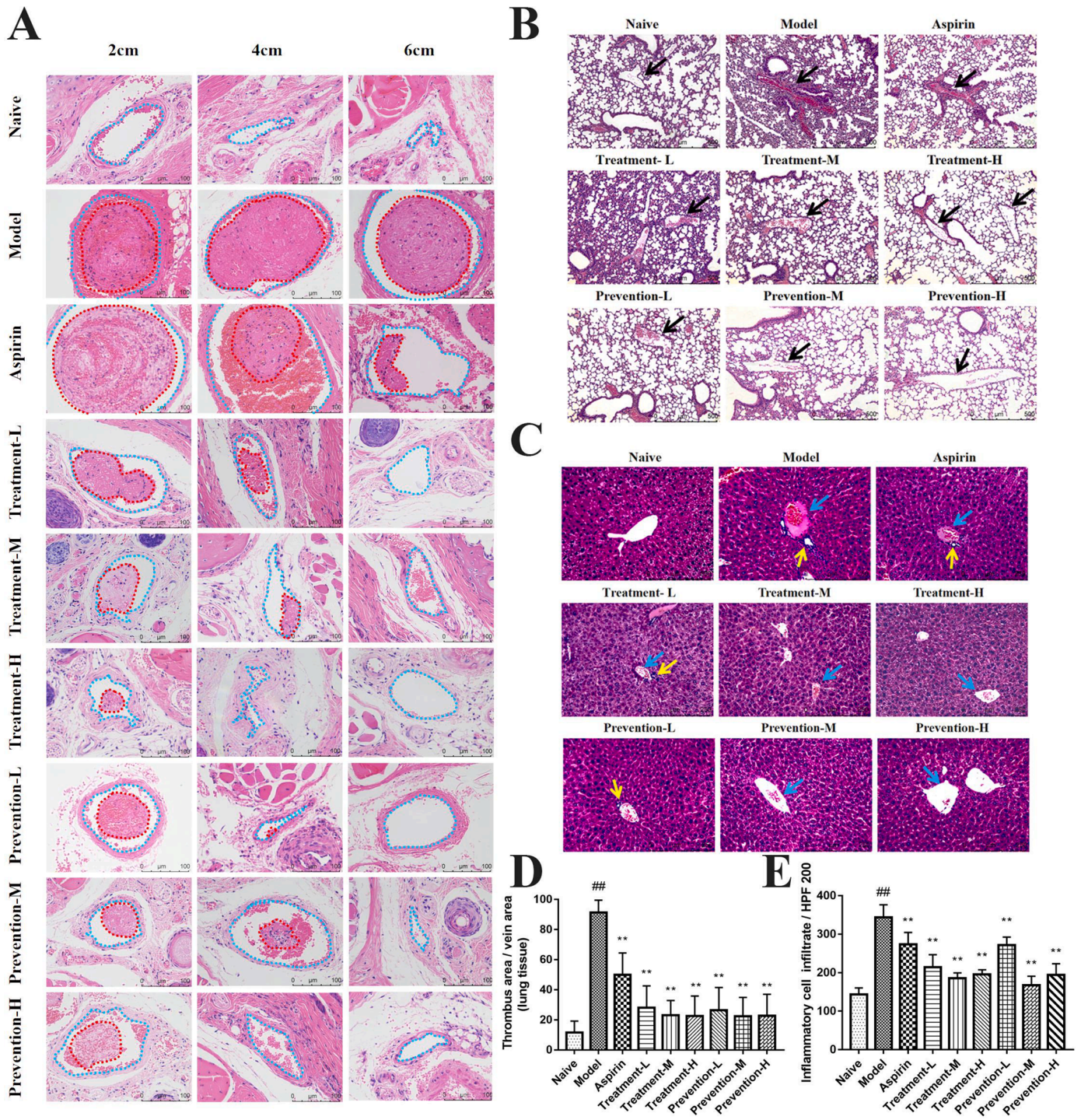

Fig 3. Effects of Gegen Qinlian pills (GQP) on carrageenan-induced thrombosis in mouse tissues. (A) Hematoxylin and eosin (HE) staining of tail at 2, 4, and 6 cm from the tail tip. Vessels and thrombi are represented by blue and red dotted lines, respectively. (B) HE staining of lung tissue. (C) HE staining of liver tissue. (D) Thrombus rate of lung tissue. (E) Inflammatory cell infiltration in liver tissue. ## $p < 0.01$ *versus* naïve group, ** $p < 0.01$ *versus* model group (n = 6).

Effects of GQP on TNF-α expression in the plasma of carrageenan-induced thrombosis mice

The level of TNF-α in the model group was markedly rised ($p < 0.01$) to 5.024 ± 0.149 pg/ml compared with the naïve group (1.967 ± 0.521 pg/ml) (Fig. 4E). After oral administration of GQP (treatment-M, prevention-M, and prevention-H) the levels of TNF-α were significantly reduced ($p < 0.05$). TNF-α levels in the aspirin group were also decreased to 3.44 ± 0.828 pg/ml, but without significant differences compared with the model group. These results suggest that GQP can inhibit carrageenan-induced TNF-α production, with a better outcome than aspirin.

Effects of GQP on the expression of HMGB1, p-NFκBp65, and NLRP3 in the lung tissue

Next, we investigated whether GQP could regulate HMGB1, p-NFκBp65, and NLRP3 expression. The results of immunohistochemical

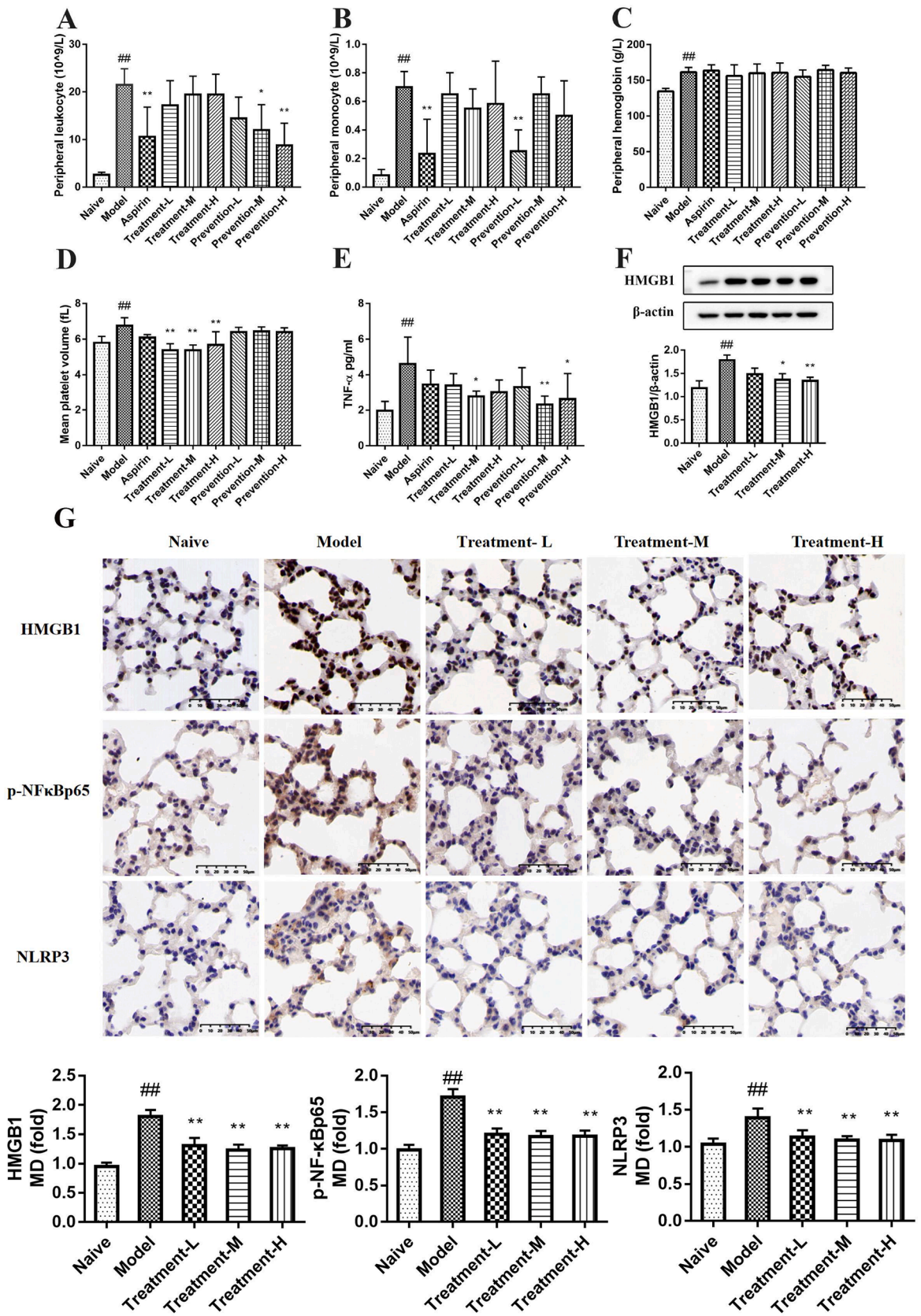

Fig. 4. Effects of Gegen Qinlian pills (GQP) on the peripheral hemogram, plasma TNF-α secretion, and HMGB1, p-NFκBp65 and NLRP3 expression in lung tissue of carrageenan-induced thrombosis mice. (A) Peripheral leukocyte count. (B) Peripheral monocyte count. (C) Peripheral hemoglobin. (D) Mean platelet volume. (E) TNF-α levels in plasma. (F) HMGB1 expression in lung tissue. (G) HMGB1, p-NFκBp65 and NLRP3 expression detected by immunohistochemistry in lung tissue. ##$p < 0.01$ *versus* naïve group, **$p < 0.01$ *versus* model group (n = 6).

showed that the expression of HMGB1, p-NFκBp65, and NLRP3 was significantly increased ($p < 0.01$) in the model group after exposure to carrageenan for 48 h, whereas GQP treatment (227.5, 445, or 910 mg/kg) decreased its expression (Fig. 4G). Western blot analysis also showed the down-regulation effect of GQP on HMGB1 (Fig. 4F). These results indicate that GQP can prevent the progression of thrombosis by suppressing HMGB1/NLRP3/NF-κB signaling.

Effects of GQP on Platelet Aggregation

We evaluated the effect of GQP on thrombin or ADP-induced platelet aggregation. Both GQP-EES 2 μg and aspirin 5 μg significantly inhibited platelet aggregation, and the inhibitory effect of aspirin on platelet aggregation was better than GQP GQP-EES 2 μg (Fig. 5).

Effects of LPS, GQP-EES, aspirin, Box A, and N4A on the viability of HUVECs

The effect of LPS, GQP-EES, aspirin, Box A, and N4A on the viability of HUVECs was detected by CCK-8 kits. Treatment with LPS (5, 10, 20, 40, 80 μg/ml) or GQP-EES (1, 2, 4, 8, 16, 32 μg/ml) or LPS (5 μg/ml) in the presence or absence of GQP-EES (1, 2, 5 μg/ml) or aspirin (10 μg/ml) with 5 μg/ml LPS or Box A (10 μg/ml) with 5 μg/ml LPS or N4A (1Mm) with 5 μg/ml LPS for 24 h has no effect on the viability of HUVECs (Fig. 6A-D).

Effects of GQP-EES on adhesion effects of LPS-treated HUVECs with platelets

To assess the effect of GQP on adhesion effects of LPS-treated HUVECs with platelets, the cells were treated with 5 μg/ml LPS to induce an inflammatory environment. Indeed, HUVECs treated with LPS significantly increased (nearly by 3-fold) platelet adhesion compared with the control group (Fig. 6E, G). GQP-EES (1, 2, or 5 μg/ml) or aspirin (10 μg/ml) treatment significantly reduced ($p < 0.01$) this effect in a dose-dependent manner.

Effects of GQP-EES on the mRNA expression of VCAM-1, ICAM-1, and vWF in LPS-treated HUVECs

The mRNA expression of VCAM-1, ICAM-1, and vWF in LPS-treated HUVEC were determined by qRT-PCR. GQP significantly ($p < 0.01$) reduced the mRNA expression of VCAM-1, ICAM-1, and vWF compared with the LPS treated group (Fig. 6H-J).

Effects of GQP-EES on the HMGB1/NF-κB/NLRP3 signaling pathway in LPS-treated HUVECs

The levels of HMGB1, NF-κBp65, p-NF-κBp65, IκBα, p-IκBα, and NLRP3 proteins were measured by Western Blotting in LPS-treated HUVECs. As shown in Fig. 7, LPS induced the expression of HMGB1, NF-κBp65, p-NF-κBp65, IκBα, p-IκBα, caspase-1 and NLRP3, whereas GQP-EES (1, 2, or 5 μg/ml) treatment markedly inhibited this effect in a dose-dependent manner. These results indicate that GQP-EES can inhibit the activation of HMGB1/NF-κB/NLRP3 signaling in LPS-induced HUVECs. Moreover, it has been observed that GQP can inhibit the translocation of NF-κBp65 to the nucleus under confocal microscope (Fig. 6F).

Effects of GQP-EES and BoxA on LPS-induced TNF-α and IL-1β production and adhesion effects of LPS-treated HUVECs with platelets

Next, we investigated the effect of the HMGB1 inhibitor BoxA and GQP-EES on the adhesion effects of LPS-treated HUVECs with platelets. Overall, GQP-EES (5 μg/ml) was found to have similar effects as BoxA (10 μg/ml), with both significantly inhibiting LPS-stimulated cell adhesion (Fig. 8A-B).

To confirm that HMGB1 overexpression contributed to TNF-α and IL-1β production, HUVECs were treated with LPS (5 μg/ml) in the presence or absence of GQP-EES (5 μg/ml) or BoxA (10 μg/ml), or GQP-EES (5 μg/ml) plus BoxA (10 μg/ml) for 24 h. TNF-α as well as IL-1β were found to be significantly increased in the LPS-treated group (Fig. 8D-E), whereas either standalone or combo GQP-EES and BoxA treatment clearly reduced ($p < 0.01$) TNF-α and IL-1β expression. Noteworthy, addition of BoxA to GQP did not further reduce TNF-α and IL-1β or platelet adhesion compared with GQP alone.

Effects of GQP-EES and BoxA on the expression of proteins of HMGB1/NF-κB/NLRP3 signaling in the LPS-treated HUVECs

Further analysis of the levels of HMGB1/NF-κB/NLRP3 signaling protein in LPS-treated HUVECs showed that the activation of pathway was enhanced by LPS, whereas GQP-EES and BoxA similarly inhibited this effect (Fig. 8C, Fig. 9).

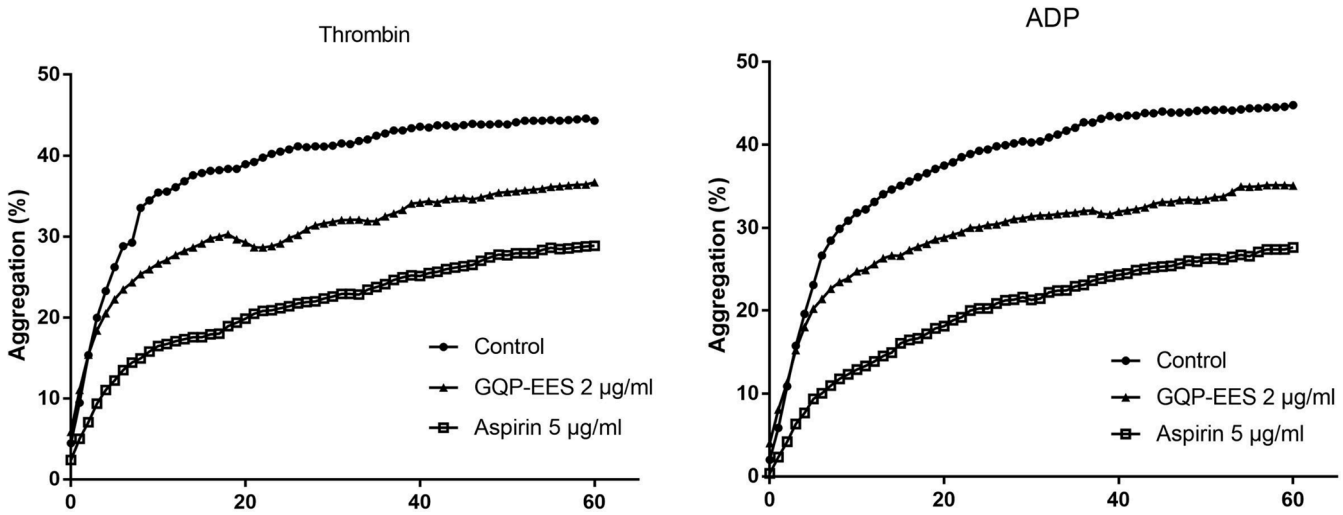

Fig. 5. Effects of Gegen Qinlian pills (GQP) on thrombin or ADP-induced platelet aggregation.The data are expressed as the mean (n=3).

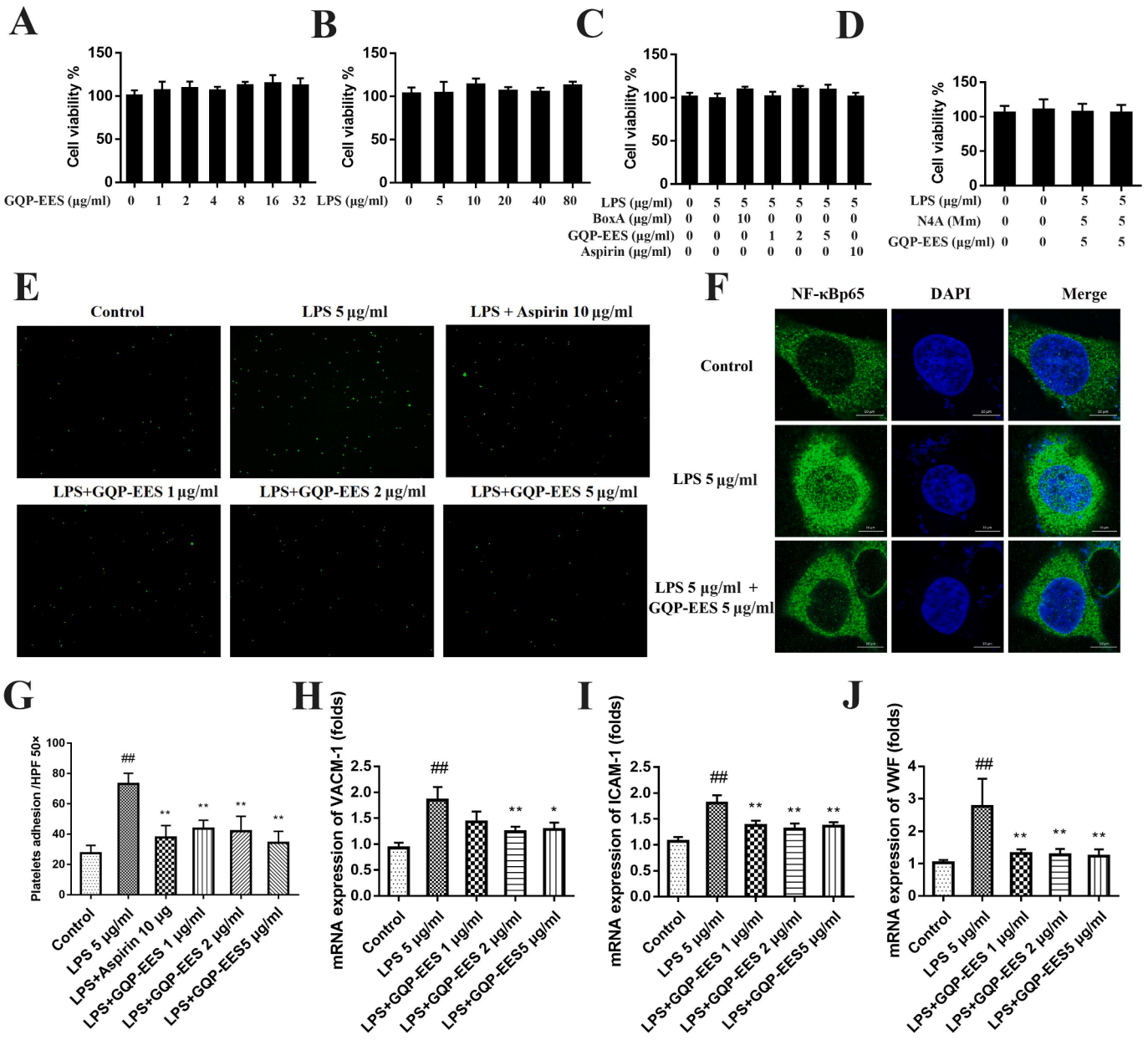

Fig. 6. Effects of Gegen Qinlian Pills ethanol extract solution (GQP-EES 1-5 μg/ml) on cell viability, platelet adhesion, NFκBp65 and mRNA expression of VCAM-1, ICAM-1, and vWF in LPS(5 μg/ml)-treated HUVECs. (A-D) Cell viability assay. (E,G) GQP-EES inhibit the adhesion of HUVECs with platelets. (F) GQP-EES inhibit the translocation of NFκBp65 observed by confocal microscopy. (H-J) GQP-EES inhibit the mRNA expression of VCAM-1, ICAM-1, and vWF. ##$p < 0.01$*versus* control group; **$p < 0.01$ and *$p < 0.05$ *versus* LPS group (n = 3).

Effects of GQP-EES and N4A on LPS-induced TNF-α and IL-1β production, adhesion effects of LPS-treated HUVECs with platelets, and the expression of proteins of HMGB1/NF-κB/NLRP3 signaling in the LPS-treated HUVECs

Further, the agonist of HMGB1, N4A was used to verify whether GQP inhibit thrombosis by inhibiting HMGB1/NF-κB/NLRP3 signaling. HUVECs were treated with LPS (5 μg/ml) in the presence or absence of GQP-EES (5 μg/ml) or GQP-EES (5 μg/ml) plus N4A (1mM) for 24 h. As we expected, the secrection of TNF-α and IL-1β, the adhesion effects of LPS-treated HUVECs with platelets, as well as the expression of HMGB1/NF-κB/NLRP3 signaling protein in LPS-treated HUVECs were up regulated and the teratment of GQP could reverse it (Fig. 10, 11). The addition of N4A counteracts the effect of GQP that could further verify GQP acting through HMGB1/NF-κB/NLRP3 signaling, inhibits thrombosis.

HPLC analysis of active components in GQP

To investigate the active components of GQP, the prepared sample was analyzed by HPLC Fig. 12. Here, we identified 10 components in GQP, including puerarin (2.78 mg/g), daidzin (1.85 mg/g), liquiritin (0.38 mg/g), genistin (94.82 μg/g), jatrorrhizine (53.57 μg/g), baicalin (0.74 mg/g), palmatine (0.84 mg/g), berberine (4.71 mg/g), wogonoside (0.27 mg/g), and glycyram (3.24 mg/g).

Molecular docking

Molecular docking simulation was performed among the 10 identified ingredients and HMGB1, using Autodock Vina1.1.2. The docking score is shown in Table 1. A lower energy always accompanied by a more stable conformation. As each binding energy of core target and component in this study was lower than -5 kcal/mol, a good docking

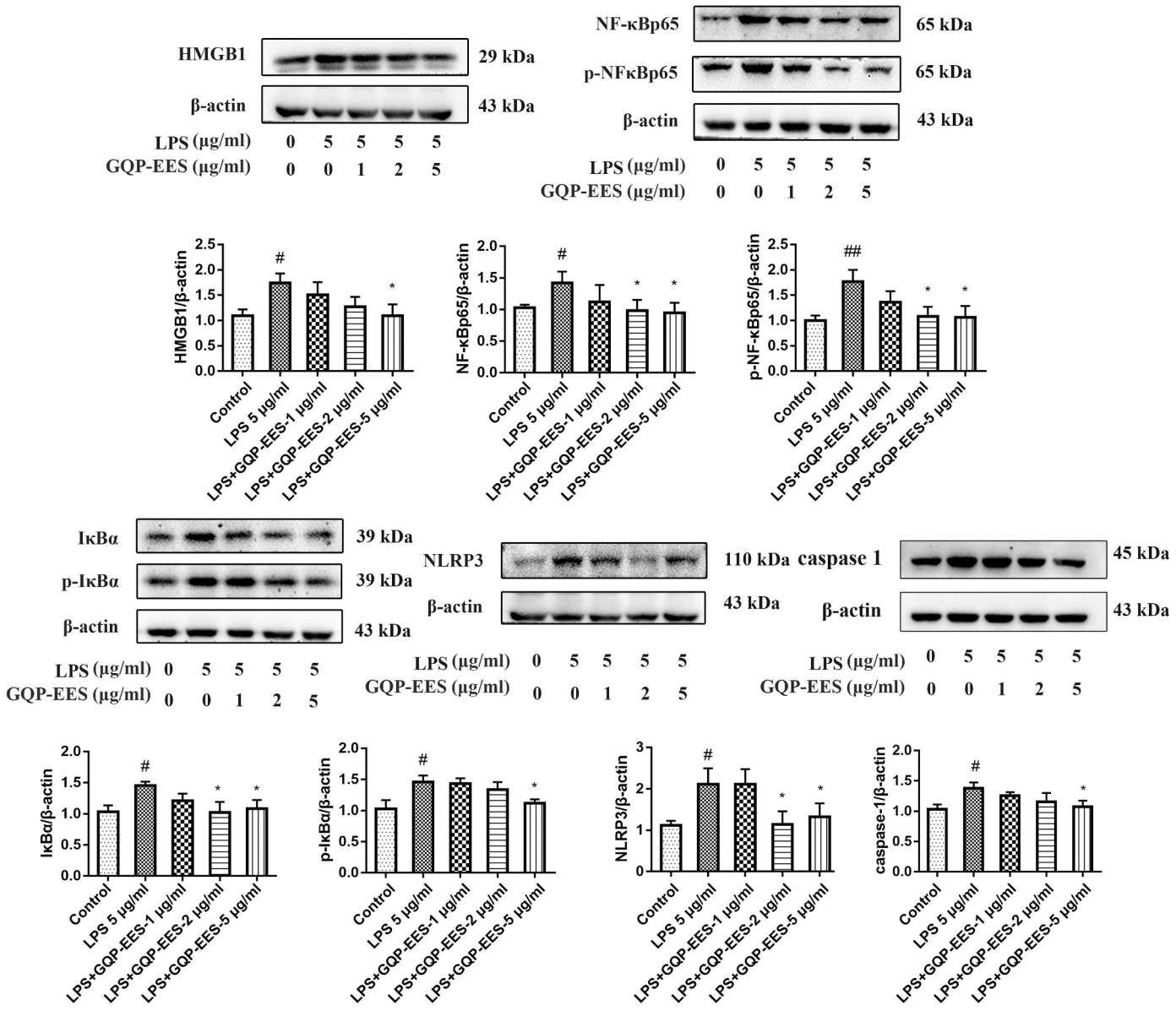

Fig. 7. Effects of Gegen Qinlian Pills ethanol extract solution (GQP-EES 1-5 μg/ml) on the expression of proteins of HMGB1/NF-κB/NLRP3 signaling in LPS (5 μg/ml)-treated HUVECs. *##p* < 0.01*versus* control group; ***p* < 0.01 and **p* < 0.05 *versus* LPS group (n = 3).

ability was predicted. Among them, wogonoside had the most stable conformation (-8 kcal/mol) with HMGB1. The partial docking process is shown in Fig. 13A.

Drug-Ingredients-Targets-Disease (D-I-T-D) Network Construction

Next, we searched targets of these 10 ingredients. After eliminating duplicates, a total of 319 compounds associated targets were identified. Moreover, a total of 454 targets related to PE were identified and 748 targets related to pneumonia were obtained, among which 66 and 68 targets of PE and pneumonia overlapped with those of GQP. Furthermore, we found 40 common targets between GQP, PE, and pneumonia. Hence, these 40 targets, which are related to both diseases, may be the key targets of GQP in the treatment of inflammation-related thrombosis.

Due to the multi-channel and multi-target features of the TCM formula, we constructed a D-I-T-D network to clarify how GQP may act against PE and pneumonia (Fig. 13B). The network consisted of 107 nodes (comprising 10 candidate ingredients, 94 potential targets, GQP and the two diseases) and 298 edges. The top three high-degree components were associated with multiple targets, namely, palmatine (degree = 26), jatrorrizine (degree = 24), genistein (degree = 23), puerarin (degree = 17), and berberine (degree = 17), which may be the key components of GQP in the treatment of inflammation-related thrombosis.

PPI, GO, and KEGG analysis

A total of 94 target proteins of GQP related to PE and pneumonia were imported into the STRING database to construct the PPI network (Fig. 13C), (combined score > 0.7). The higher the degree the targets were bigger. Ultimately, AKT1, STAT3, MAPK1, TP53, and VEGFA with a degree value of > 40, were identified as key nodes, suggesting that they may play key role in the treatment of inflammation-related thrombosis.

The first 20 terms of the biological process of GQP in the treatment of inflammation-related thrombosis are shown by significance (from small to large *p*-value) in Fig. 13D. Including protein tyrosine kinase activity (n = 16), transmembrane receptor protein kinase activity (n = 13), and

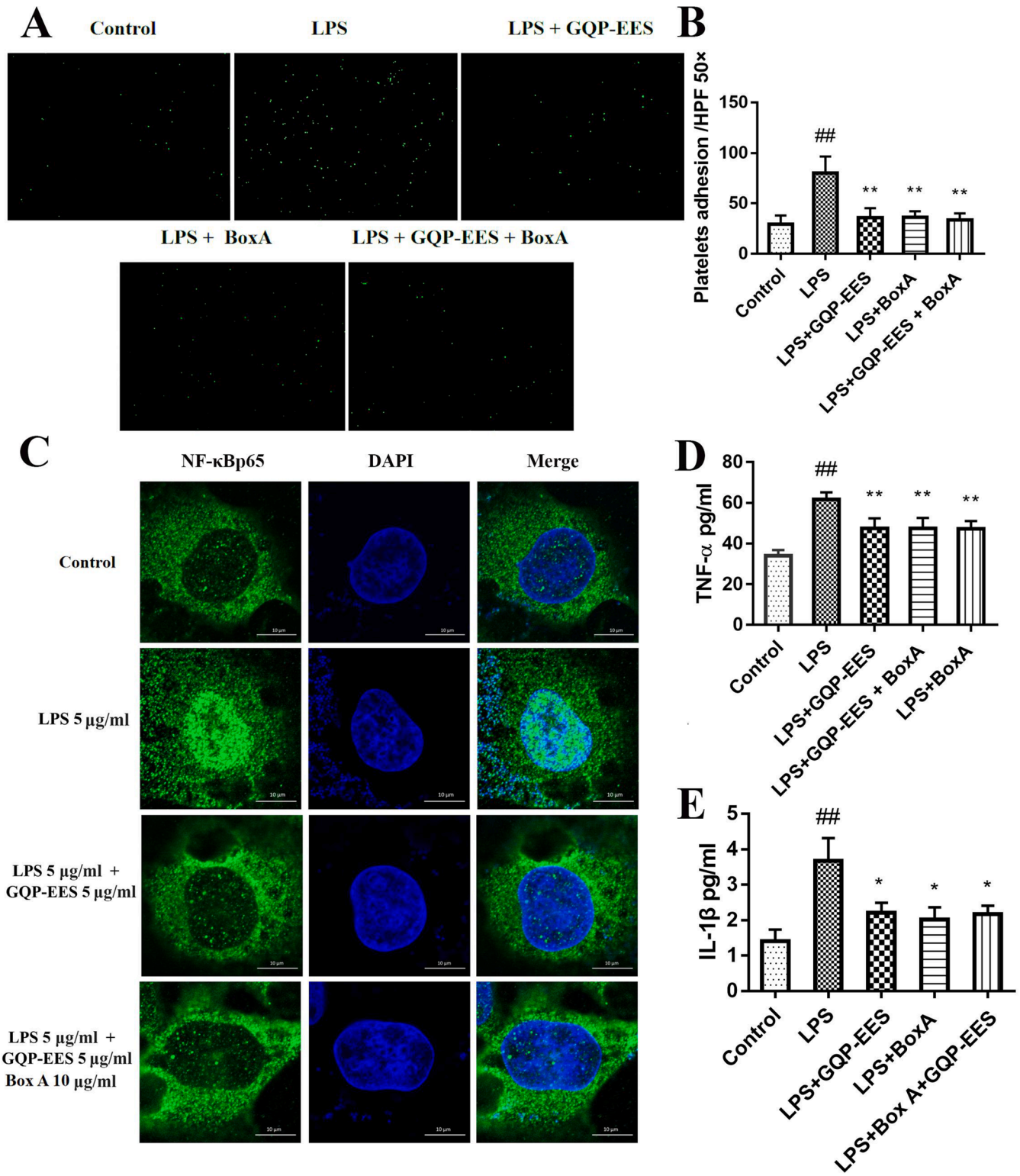

Fig. 8. Effects of GQP-EES (5 μg/ml) and BoxA (10 μg/ml) on platelet adhesion, NFκBp65 translocation and TNF-α and IL-1β production in LPS (5 μg/ml)-treated HUVECs. (A-B) Platelets adhesion assay. (C) NFκBp65 translocation under confocal microscopy. (D-E) Effects of GQP-EES and BoxA on TNF-α and IL-1β production. ##$p < 0.01$ *versus* control group; **$p < 0.01$ and *$p < 0.05$ *versus* LPS group (n = 3).

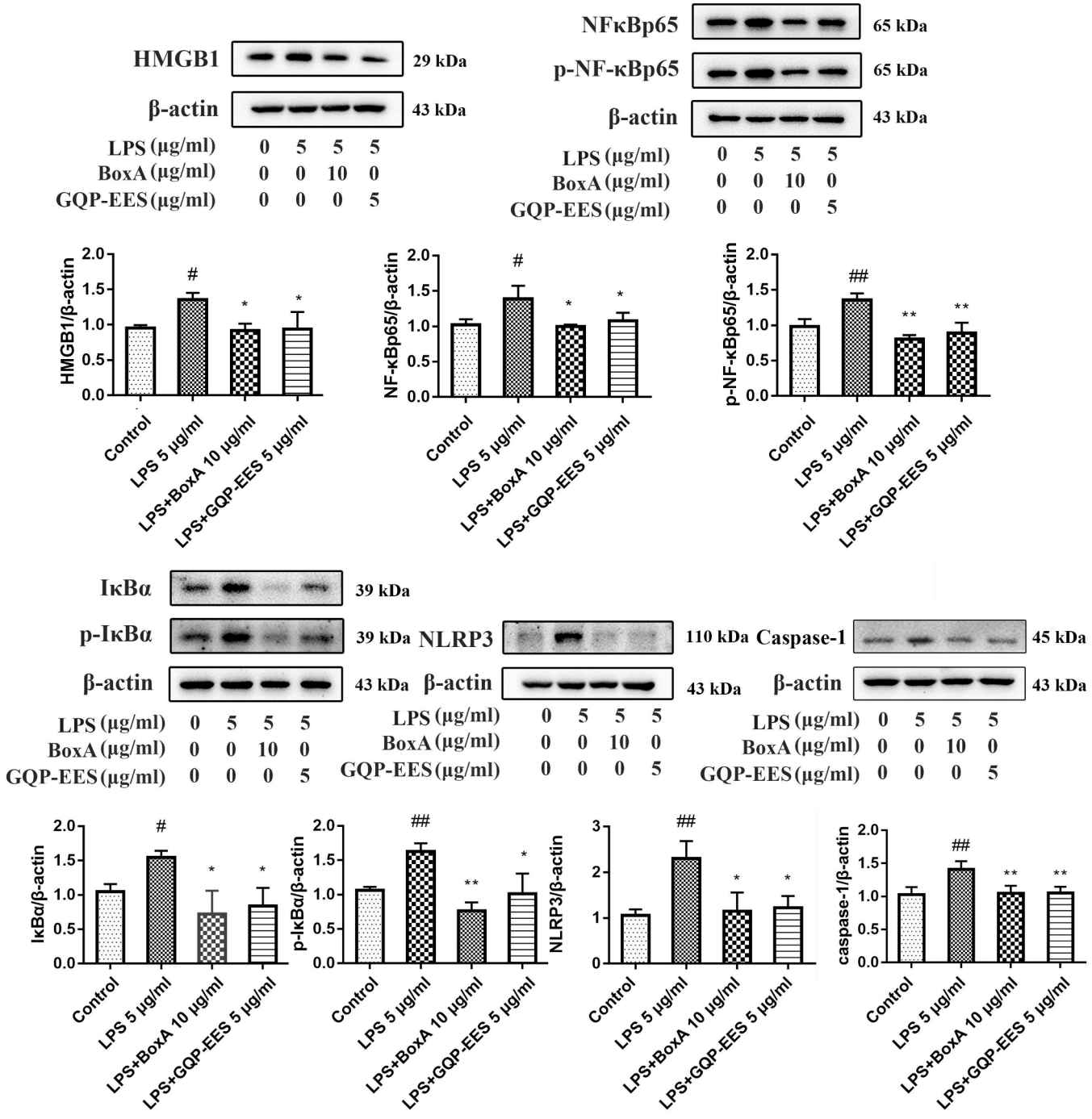

Fig. 9. Effects of GQP-EES (5 μg/ml) and BoxA (10 μg/ml) expression of HMGB1/NF-κB/NLRP3 signaling proteins. ##$p < 0.01$ *versus* control group; **$p < 0.01$ and *$p < 0.05$ *versus* LPS group (n = 3).

protein phosphatase binding (n = 13), suggesting that GQP may play a role in the treatment of inflammation-related thrombosis through multiple biological processes.

KEGG analysis further revealed 156 pathways related to GQP. The top 20 pathways, sorted from small to large according to p-value, are shown in Fig. 13E. These target proteins were mainly involved in AGE/RAGE, PI3K/Akt, TNF, MAPK, and Th17 cell differentiation signaling pathways, further suggesting that GQP may play a role through multiple channels in the treatment of inflammation-related thrombosis.

Discussion

It is known that COVID-19 can lead to a severe acute respiratory syndrome, increase the incidence of morbidity and mortality due to multiple organ involvement. It has been associated with an increased risk of VTE, which can be fatal (Chopra et al., 2021; Goddard et al., 2021). High levels of inflammatory cytokines such as TNF-α seem to indicate an increased risk of thrombotic events and even death in the course of COVID-19 (Rad et al., 2021). GQP has antiviral and anti-inflammatory activities, which have good effects in treating COVID-19, showing the potential of anti thrombosis. However, there is no study on the effect of GQP on thrombosis. In this study, we used an

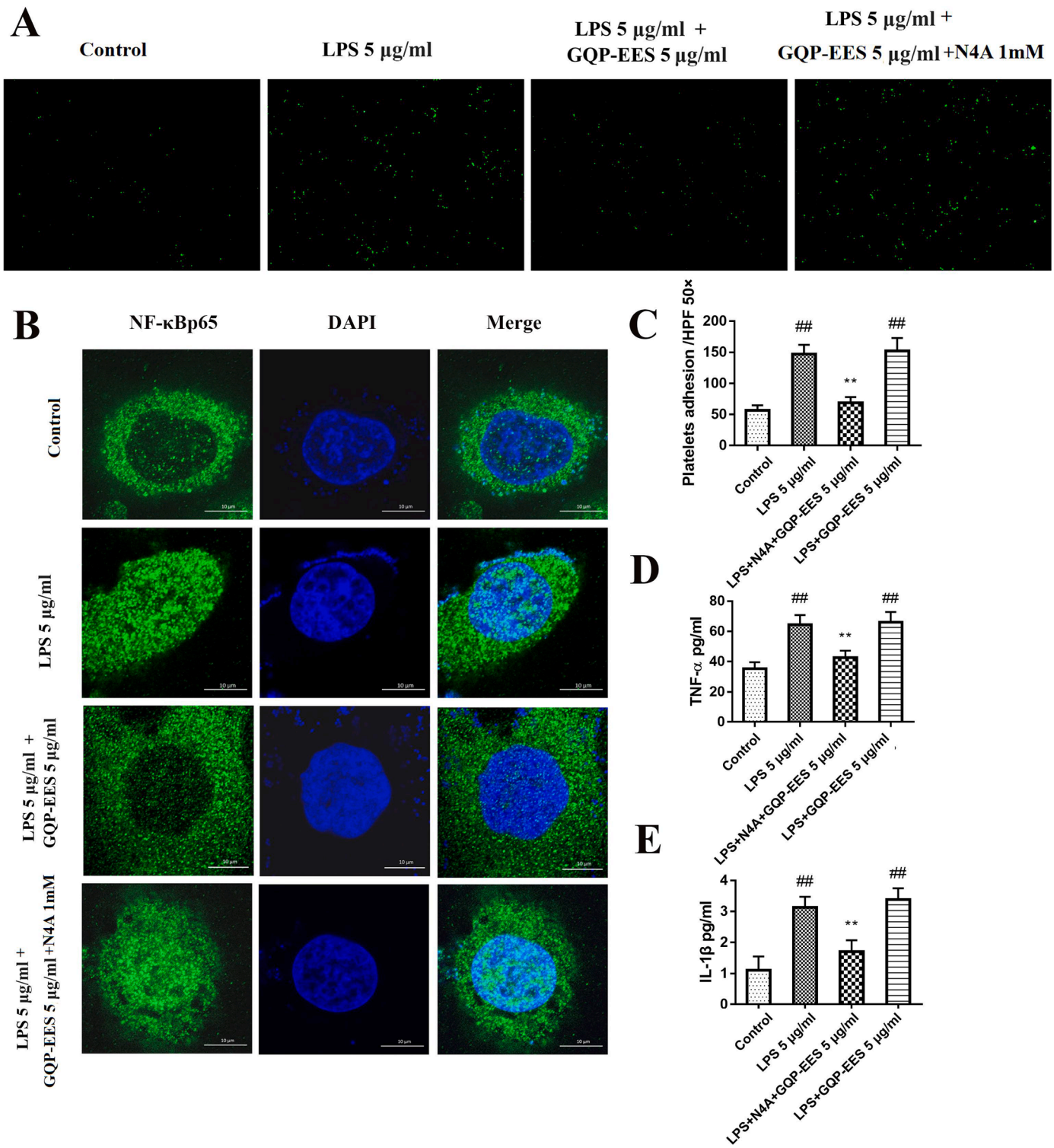

Fig. 10. Effects of GQP-EES (5 μg/ml) and N4A (1 mM) on platelet adhesion, NFκBp65 translocation and TNF-α and IL-1β production in LPS (5 μg/ml)-treated HUVECs. (A,C) Platelets adhesion assay. (B) NFκBp65 translocation under confocal microscopy. (D-E) Effects of GQP-EES and N4A on TNF-α and IL-1β production. $\#\#p < 0.01$*versus* control group; $^{**}p < 0.01$ and $^{*}p < 0.05$ *versus* LPS group (n = 3).

carrageenan-induced thrombosis mice model and treated with GQP before or after carrageenan injection to elevulate the inhibitory effect of GQP on inflammation-induced thrombus. *In vitro*, we investigated the effect of GQP and aspirin on LPS stimulated HUVEC cells on platelet adhesion and thrombin or ADP-induced platelet aggregation. We also analyzed the components of GQP and inferred the main components of its anti-inflammatory and antithrombotic effects. We demonstrated that both prophylactic and therapeutic administration of GQP inhibited carrageenan-induced thrombosis. *In vitro,* GQP inhibited the adhesion of platelets to LPS stimulated HUVEC cells and platelet aggregation. The results of the WB analysis suggest that GQP may play an anti-inflammatory role by inhibiting the HMGB1 signal, which is similar to that of the HMGB1 inhibitor BoxA. Wogonoside, puerarin, and glycyram in GQP may be the main active component in inhibiting HMGB1.

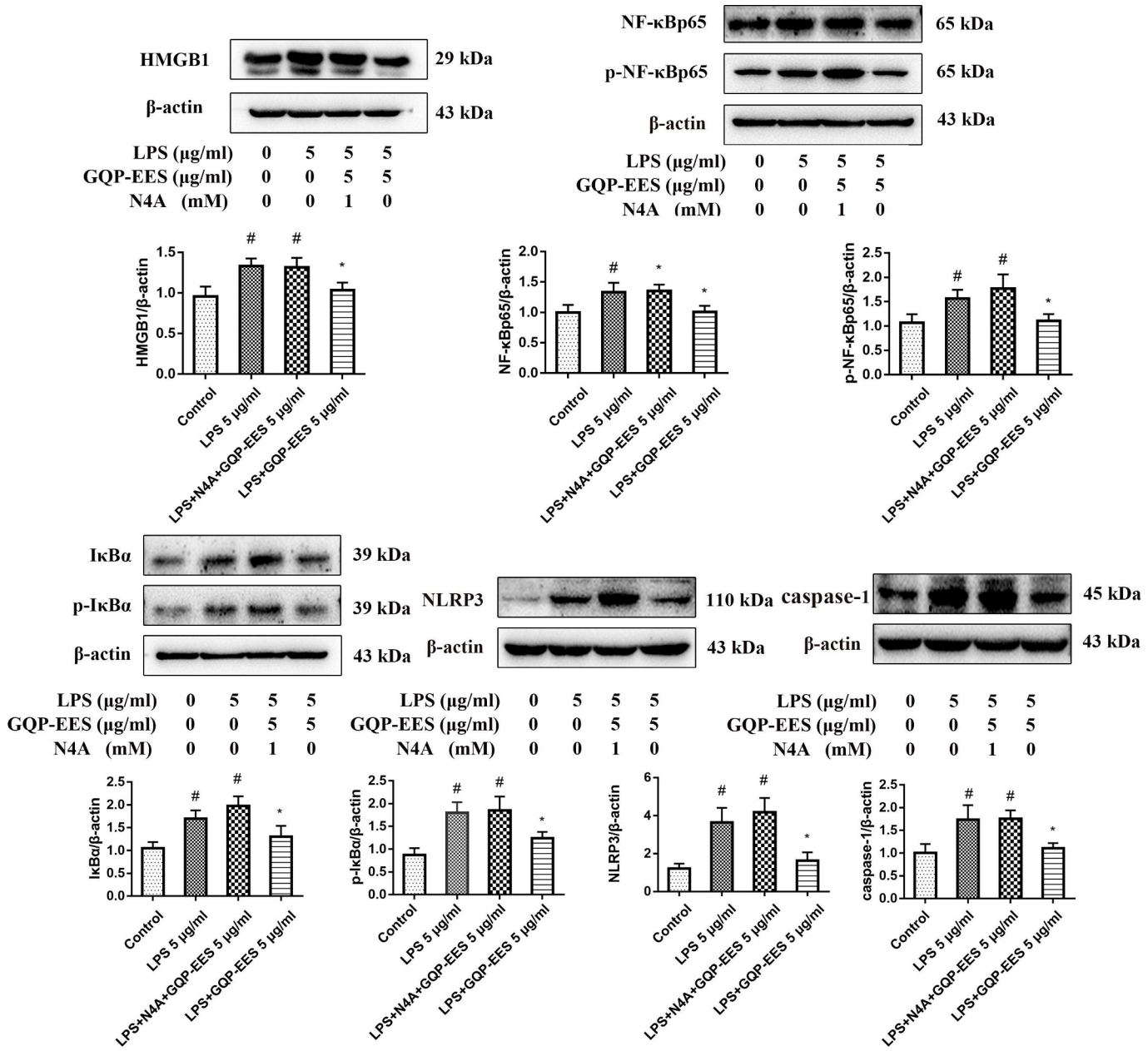

Fig. 11. Effects of GQP-EES (5 μg/ml) and N4A (1mM) expression of HMGB1/NF-κB/NLRP3 signaling proteins. #$p < 0.05$ *versus* control group; *$p < 0.05$ *versus* LPS group (n = 3).

GQP affected various targets and has synergistic effects and therapeutic multi-pharmacology in the treatment of inflammation-induced thrombosis.

Carrageenan is a linear sulfur-containing macromolecular polysaccharide, that is widely used in the model of thrombosis. It can cause inflammation in local blood vessels, lead to the secretion of inflammatory factors, damage vascular endothelial cells, and cause thrombosis (Kim et al., 2021). Therefore, in this study, we used the carrageenan-induced thrombus model to evaluate the effect of GQP on inflammation-induced thrombus. The peripheral leukocyte count, monocyte count, and plasma TNF-α in the model group were significantly increased, which indicated that carrageenan caused a systemic inflammatory response. Aspirin is a potent inhibitor of platelet enzyme cyclooxygenase 1 (COX-1), which is widely used in the clinic to prevent cardiovascular thrombosis events. However, regular use of aspirin may lead to gastrointestinal toxicity, including hemorrhage, ulcers, and perforation (Varga et al., 2016). Thus, it is necessary to develop new thrombolytic drugs with fewer side effects. The results of our experiments showed that GQP had better effects than aspirin in reducing tail thrombotic length, and TNF-α in plasma. Interestingly, while aspirin is widely used to prevent platelet aggregation and thrombogenesis, the blood flow and the tail thrombus length were no significant difference ($p > 0.05$) between the aspirin and model groups in our study. There are several studies that consistent with our results, this may be because carrageenan damage vascular endothelial cells that maintain coagulation and fibrinolysis by causing inflammation, thereby causing thrombus, platelet activation played only a partial role in this model, antiaggregant is different from antithrombotic (Arslan et al., 2011; Gervasi et al., 1991; Ma et al., 2015). Moreover, the mean tail thrombotic length in the GQP medium-dose group (445 mg/kg) was shorter rather than in the low (227.5 mg/kg) and high (910 mg/kg) dose groups. A similar trend was also reported when GQP was used to treat xenograft tumors in mice (Lv et al., 2019). The underlying mechanisms need to be further explored.

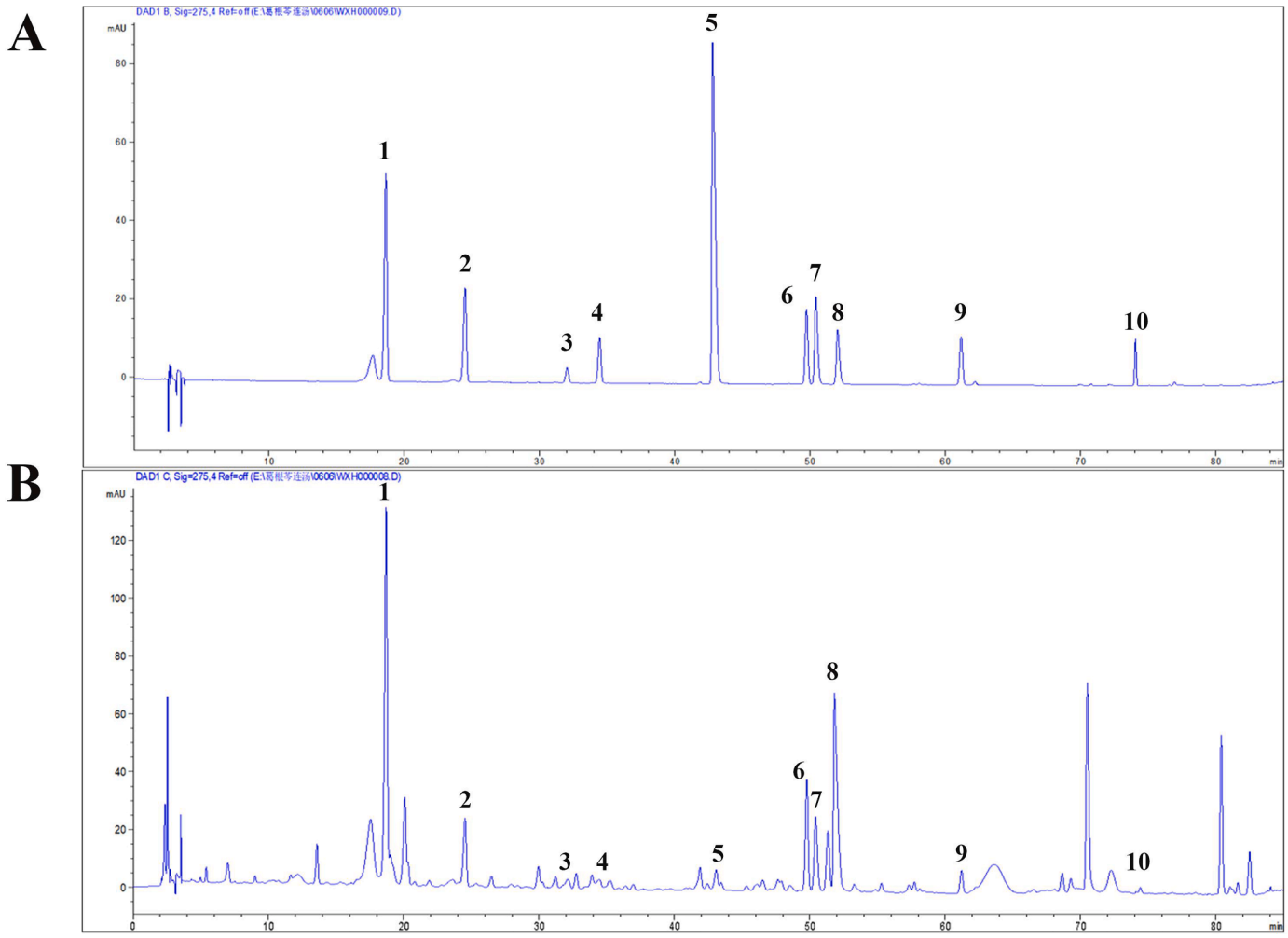

Fig. 12. The HPLC chromatograms of ethanol extract from Gegen Qinlian pills at 275 nm; (A). HPLC chromatograms of the standard references. (B). HPLC chromatograms of ethanol extract from Gegen Qinlian Pills. 1-puerarin, 2-daidzin, 3-liquiritin, 4-genistin, 5-jatrorrhizine, 6-baicalin, 7-palmatine, 8-berberine, 9-wogonoside, 10- glycyram.

Table 1
The molecular docking results

Protein	Test compounds	Affinity (kcal/mol)
HMGB1 (PDB code 2YRQ)	wogonoside	-8
	puerarin	-7.7
	glycyram	-7.6
	berberine	-7.6
	baicalin	-7.5
	genistin	-7.3
	daidzin	-7.3
	palmatine	-7.1
	jatrorrhizine	-6.8
	liquiritin	-6.6

TNF-α is a multifunctional cytokine that is very important in immune regulation, inflammation, thrombosis, and tumor metastasis (Bradley, 2008). It can activate vascular endothelial cells, promote platelet hyperactivity, and thus induce the formation of venous thrombosis (Satta et al., 2011). TNF-α stimulates the TNF receptor (TNFR) and induces the phosphorylation of IκB kinase (IKK), which induces NF-κB activity (Zhang et al., 2017). In our study, GQP treatment significantly decreased the TNF-α levels in mice plasma, and the supernatant of HUVECs, as well as the expression of NLRP3 and NF-κB. These results suggest that the anti-thrombosis effect of GQP may be related to the inhibition of TNF-α.

NF-κB plays a crucial role in inflammation, as it can regulate DNA transcription, cytokine production, and cell survival, being active in PE, acute lung injury, and many other inflammatory diseases (Liang et al., 2021; Lu et al., 2018; Lu et al., 2020). The phosphorylation of IκBα can induce NF-κB dimers to actively shuttle between the nucleus and the cytosol, inducing gene expression (Zhang et al., 2017). In this study, the generation of HMGB1 and activation of NF-κB and NLRP3 was observed in different groups. Noteworthy, GQP was able to reduce HMGB1, NF-κB, and NLRP3 in the lung tissue which at least partially support the hypothesis that GQP can inhibit inflammation-induced thrombosis by suppressing HMGB1/NF-κB/NLRP3 signaling.

Vascular endothelial cells are the first barrier between the tissues and blood, hence, damage to vascular endothelial cells is the first step of arteriovenous thrombosis (Iba and Levy, 2018). It is reported that TNF-α or LPS can stimulate endothelial cells to release HMGB1, which is turn can also stimulate endothelial cells to secrete TNF-α (Lee et al., 2017; Luan et al., 2010). Therefore, HMGB1 and TNF-α can aggravate the damage of vascular endothelial cells and promote the secretion of von Willebrand factor (VWF), NLRP3, and the expression of P-selectin thus promoting thrombosis (Jia et al., 2019; Singh et al., 2016). NLRP3 and HMGB1 are also the regulators of platelet aggregation (Vogel and Thein, 2018). In this study, GQP-EES significantly inhibited the adhesion of platelets to LPS-stimulated HUVECs and TNF-α and IL1-β production, it also diminished the expression of HMGB1, NF-κB, IκBα, caspase1, and NLRP3 in these cells. BoxA is a specific blocker for HMGB1, which was proved to downregulate LPS-induced proinflammatory cytokines, such

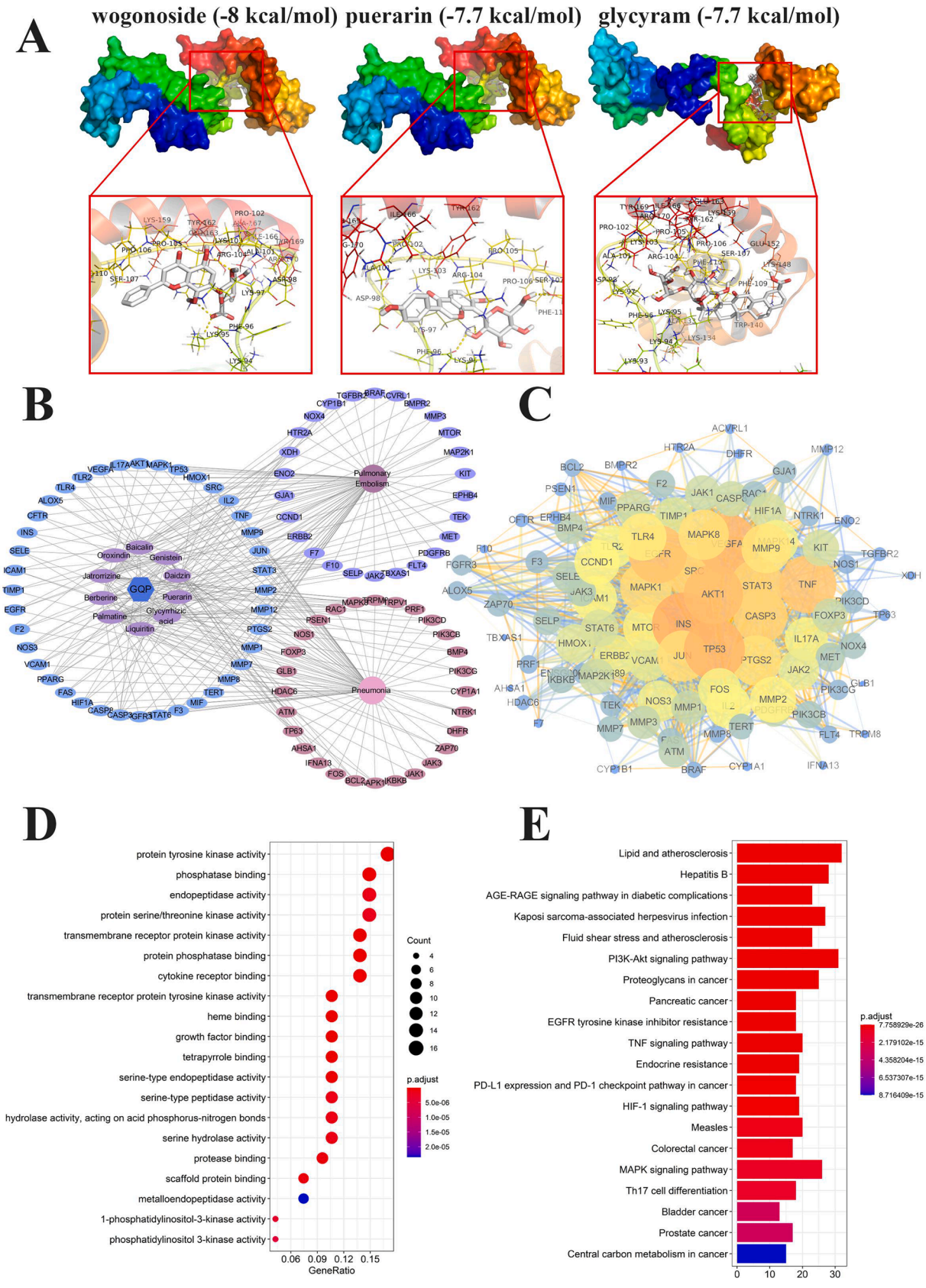

Fig. 13. Molecular docking and network pharmacology analysis. (A) Molecular docking process of HMGB1 with wogonoside, puerarin, and glycyram, respectively. (B) Drug-Ingredients-Targets-Disease (D-I-T-D) Network of Gegen Qinlian pills (GQP). (C) Protein–protein interaction (PPI) network of 94 targets of GQP in pulmonary embolism and pneumonia. (D) GO and (E) KEGG pathway enrichment analyses of the 94 targets of GQP in pulmonary embolism and pneumonia.

as early mediator TNF-α and late mediator HMGB1 (Gong et al., 2009). N4A is an agonist of HMGB1, which can activate NLRP3 by increasing the expression of HMGB1 (Duan et al., 2019). Similar results were observed in our experiments, BoxA has reduced the expression of HMGB1, NF-κB, IκBα, and NLRP3 and TNF-α expression in LPS-stimulated HUVECs. However, addition of BoxA to GQP did not further reduce TNF-α levels or platelet adhesion compared with GQP alone, and the addition of N4A counteracts the effect of GQP. Therefore, we believe that BoxA and GQP exert a similar effect on LPS-stimulated HUVECs, with GQP exerting its antithrombotic effect (at least partly) by inhibiting HMGB1.

HPLC analysis revealed 10 components of GQP, which were used to perform molecular docking and bioinformatics analyses on GQP. The top five components with the lowest binding energy were wogonoside, puerarin, glycyram, berberine, and baicalin. It has been demonstrated that glycyram is a potent inhibitor of HMGB1 (Paudel et al., 2021), which indicates that our prediction is reliable. Wogonoside, puerarin, glycyram, berberine, and baicalin may also be antagonists of HMGB1, which will be explored in future studies.

Moreover, in order to further explore other possible mechanisms of GQP in the treatment of inflammation-related thrombosis, we conducted a bioinformatics analysis. We got 94 target proteins of GQP that related to PE and pneumonia. These targets play an important role in the pathogenesis of thrombosis, including protein tyrosine kinase activity (Totzeck et al., 2018), transmembrane receptor protein kinase activity (Guzik et al., 2020), and protein phosphatase binding (Inamdar et al., 2019). Key targets AKT1, STAT3, MAPK1, TP53, and VEGFA are all involved in thrombosis. As Chen et al (2005) reported, the Akt-thrombospondin axis plays a crucial role in angiogenesis; Moreover, suppression of STAT3 expression can prevent lower extremity DVT in peripheral blood, and activation of the MAPK pathway can also mediate platelet activation (Zhang et al., 2020). In addition, TP53 can affect the number of platelets by interacting with various genes (Cerquozzi and Tefferi, 2015), and reduced VEGFA levels are associated with an increased risk of thrombosis (Candan et al., 2014). Herein, KEGG enrichment analysis showed that the GQP therapeutic effects on inflammation-related thrombosis are mainly related to the AGE/RAGE, PI3K/Akt, TNF, and MAPK signaling pathways. The AGE/RAGE, PI3K/Akt signaling pathway can attenuate the activation of platelets (Chen et al., 2019; Recabarren-Leiva et al., 2021). Ding et al (2020) reported that Gegen Qinlian decoction can against LPS-induced acute lung injury by activating PI3K/Akt signals and downregulating the secretion of LPS-induced TNF-α in lung tissue. Activation of the TNF signaling pathway can trigger and aggravate vascular endothelial cell injury (Hou et al., 2019). In our study, GQP diminished the expression of TNF-α in plasma and in the supernatant of HUVECs. MAPK signaling pathway is not only closely related to an inflammatory reaction but also affects thromboxane production and thrombosis in platelets (Manne et al., 2018; Yong et al., 2009). In general, Traditional Chinese medicine formula has the characteristics of multi-target, multi-function, and multi-pathway therapeutic function. The results of bioinformatics analysis indicate that the effect of GQP on thrombosis has synergistic effects and therapeutic multi-pharmacology.

However, there are still some research deficiencies in this study. In the animal experiment, the animal was limited in scale, and the positive drug group was only set in the prevention group; Since this study mainly discusses the effect of GQP on vascular endothelial cells, we have not conducted an in-depth study on the activation mechanism of GQP on platelets. Moreover, when studying the mechanism of GQP in the treatment of thrombosis, we only used HMGB1 inhibitor BoxA and activator N4A for comparison. Additional studies using gene knockdown or overexpression strategies should be performed in the future to validate our findings.

In conclusion, it's the first time that GQP had demonstrated reducing inflammation-induced thrombosis *in vivo* and attenuating platelet adhesion *in vitro* by suppressing HMGB1/NFκB/NLRP3 signaling. These findings suggest that GQP is a potential candidate in treating inflammation-induced thrombosis and provides a reference for the clinical usage of GQP.

Author contributions and CRediT author statement

X.H. Wei wrote the paper draft, X.M. Tan corrected the draft. X.H. Wei and B.P. Zhang mainly conducted this study. M.Z. Ding and Z.Y. Luo provided help on animal handling. X.L. Han supervised the experimentators. X.M. Tan provided funding to support the study. All data were generated in-house, and no paper mill was used. All authors agree to be accountable for all aspects of work ensuring integrity and accuracy.

Conflict of Interest

The authors have no conflicts to declare.

Acknowledgments

This work was supported by the Natural Science Foundation of Guangdong Province (grant number 2019A1515011398), the National Natural Science Foundation of China (grant number 8197141413).

References

Al-Samkari, H., Karp, L.R., Dzik, W.H., Carlson, J., Fogerty, A.E., Waheed, A., Goodarzi, K., Bendapudi, P.K., Bornikova, L., Gupta, S., Leaf, D.E., Kuter, D.J., Rosovsky, R.P., 2020. COVID-19 and coagulation: Bleeding and thrombotic manifestations of SARS-CoV-2 infection. Blood 136, 489–500.

Arslan, R., Bor, Z., Bektas, N., Meriçli, A.H., Ozturk, Y., 2011. Antithrombotic effects of ethanol extract of Crataegus orientalis in the carrageenan-induced mice tail thrombosis model. Thromb Res 127, 210–213.

Biswas, I., Khan, G.A., 2020. Coagulation disorders in COVID-19: Role of toll-like receptors. J Inflamm Res 13, 823–828.

Bradley, J.R., 2008. TNF-mediated inflammatory disease. J Pathol 214, 149–160.

Candan, F., Yildiz, G., Kayataş, M., 2014. Role of the VEGF 936 gene polymorphism and VEGF-A levels in the late-term arteriovenous fistula thrombosis in patients undergoing hemodialysis. Int Urol Nephrol 46, 1815–1823.

Cerquozzi, S., Tefferi, A., 2015. Blast transformation and fibrotic progression in polycythemia vera and essential thrombocythemia: A literature review of incidence and risk factors. Blood Cancer J 5, e366.

Chen, J., Somanath, P.R., Razorenova, O., Chen, W.S., Hay, N., Bornstein, P., Byzova, T. V., 2005. Akt1 regulates pathological angiogenesis, vascular maturation and permeability *in vivo*. Nat Med 11, 1188–1196.

Chen, Z., Li, T., Kareem, K., Tran, D., Griffith, B.P., Wu, Z.J., 2019. The role of PI3K/Akt signaling pathway in non-physiological shear stress-induced platelet activation. Artif Organs 43, 897–908.

Choo, M.K., Park, E.K., Yoon, H.K., Kim, D.H., 2002. Antithrombotic and antiallergic activities of daidzein, a metabolite of puerarin and daidzin produced by human intestinal microflora. Biol Pharm Bull 25, 1328–1332.

Chopra, S., Kaur, J., Kaur, M., 2021. Massive pulmonary embolism and deep vein thrombosis in COVID-19 pneumonia: Two case reports. Cureus 13, e14833.

Ding, Z., Zhong, R., Yang, Y., Xia, T., Wang, W., Wang, Y., Xing, N., Luo, Y., Li, S., Shang, L., Shu, Z., 2020. Systems pharmacology reveals the mechanism of activity of Ge-Gen-Qin-Lian decoction against LPS-induced acute lung injury: A novel strategy for exploring active components and effective mechanism of TCM formulae. Pharmacol Res 156, 104759.

Duan, J., Zhang, Q., Hu, X., Lu, D., Yu, W., Bai, H., 2019. N(4)-acetylcytidine is required for sustained NLRP3 inflammasome activation via HMGB1 pathway in microglia. Cell Signal 58, 44–52.

Engelmann, B., Massberg, S., 2013. Thrombosis as an intravascular effector of innate immunity. Nat Rev Immunol 13, 34–45.

Gervasi, G.B., Bartoli, C., Carpita, G., 1991. A new low molecular weight heparan sulphate antagonizes kappa-carrageenan-induced thrombosis in rats. Pharmacol Res 24, 59–63.

Goddard, S.A., Tran, D.Q., Chan, M.F., Honda, M.N., Weidenhaft, M.C., Triche, B.L., 2021. Pulmonary vein thrombosis in COVID-19. Chest 159, e361–e364.

Gong, Q., Xu, J.F., Yin, H., Liu, S.F., Duan, L.H., Bian, Z.L., 2009. Protective effect of antagonist of high-mobility group box 1 on lipopolysaccharide-induced acute lung injury in mice. Scand J Immunol 69, 29–35.

Guzik, T.J., Mohiddin, S.A., Dimarco, A., Patel, V., Savvatis, K., Marelli-Berg, F.M., Madhur, M.S., Tomaszewski, M., Maffia, P., D'Acquisto, F., Nicklin, S.A., Marian, A. J., Nosalski, R., Murray, E.C., Guzik, B., Berry, C., Touyz, R.M., Kreutz, R., Wang, D. W., Bhella, D., Sagliocco, O., Crea, F., Thomson, E.C., McInnes, I.B., 2020. COVID-19 and the cardiovascular system: Implications for risk assessment, diagnosis, and treatment options. Cardiovasc Res 116, 1666–1687.

Hou, X., Yang, S., Yin, J., 2019. Blocking the REDD1/TXNIP axis ameliorates LPS-induced vascular endothelial cell injury through repressing oxidative stress and apoptosis. Am J Physiol Cell Physiol 316, C104–C110.
Iba, T., Levy, J.H., 2018. Inflammation and thrombosis: Roles of neutrophils, platelets and endothelial cells and their interactions in thrombus formation during sepsis. J Thromb Haemost 16, 231–241.
Inamdar, V.V., Kostyak, J.C., Badolia, R., Dangelmaier, C.A., Manne, B.K., Patel, A., Kim, S., Kunapuli, S.P., 2019. Impaired glycoprotein VI-Mediated signaling and platelet functional responses in CD45 knockout mice. Thromb Haemost 119, 1321–1331.
Jia, C., Zhang, J., Chen, H., Zhuge, Y., Chen, H., Qian, F., Zhou, K., Niu, C., Wang, F., Qiu, H., Wang, Z., Xiao, J., Rong, X., Chu, M., 2019. Endothelial cell pyroptosis plays an important role in Kawasaki disease via HMGB1/RAGE/cathespin B signaling pathway and NLRP3 inflammasome activation. Cell Death Dis 10, 778.
Katneni, U.K., Alexaki, A., Hunt, R.C., Schiller, T., DiCuccio, M., Buehler, P.W., Ibla, J.C., Kimchi-Sarfaty, C., 2020. Coagulopathy and thrombosis as a result of severe COVID-19 infection: A microvascular focus. Thromb Haemost 120, 1668–1679.
Kim, E.S., Lee, J.S., Lee, H.G., 2021. Improvement of antithrombotic activity of red ginseng extract by nanoencapsulation using chitosan and antithrombotic cross-linkers: Polyglutamic acid and fucodian. J Ginseng Res 45, 236–245.
Kim, S.W., Lee, J.K., 2020. Role of HMGB1 in the interplay between NETosis and thrombosis in ischemic stroke: A review. Cells-Basel 9.
Klok, F.A., Kruip, M., van der Meer, N., Arbous, M.S., Gommers, D., Kant, K.M., Kaptein, F., van Paassen, J., Stals, M., Huisman, M.V., Endeman, H., 2020. Incidence of thrombotic complications in critically ill ICU patients with COVID-19. Thromb Res 191, 145–147.
Lee, W., Ku, S.K., Bae, J.S., 2017. Zingerone reduces HMGB1-mediated septic responses and improves survival in septic mice. Toxicol Appl Pharmacol 329, 202–211.
Li, Q., Chen, Y., Zhao, D., Yang, S., Zhang, S., Wei, Z., Wang, Y., Qian, K., Zhao, B., Zhu, Y., Chen, Y., Duan, Y., Han, J., Yang, X., 2019. LongShengZhi Capsule reduces carrageenan-induced thrombosis by reducing activation of platelets and endothelial cells. Pharmacol Res 144, 167–180.
Li, R., Chen, Y., Shi, M., Xu, X., Zhao, Y., Wu, X., Zhang, Y., 2016. Gegen Qinlian decoction alleviates experimental colitis via suppressing TLR4/NF-κB signaling and enhancing antioxidant effect. Phytomedicine 23, 1012–1020.
Liang, D., Wen, Z., Han, W., Li, W., Pan, L., Zhang, R., 2021. Curcumin protects against inflammation and lung injury in rats with acute pulmonary embolism with the involvement of microRNA-21/PTEN/NF-κB axis. Mol Cell Biochem 476, 2823–2835.
Linqun, W., Weinan, L., Wei, H., Zhouming, Z., Yali, D., Yunlian, H., Ran, T., Xinhe, Z., Bianbian, Yi, F., Dingbo, L., Bianbian, Y., 2020. Clinical study of Gegen Qinlian pill in treating COVID-19. Modernization of Traditional Chinese Medicine and Materia Medica-World Science and Technology 22, 3509–3514.
Lu, Z., Xie, P., Zhang, D., Sun, P., Yang, H., Ye, J., Cao, H., Huo, C., Zhou, H., Chen, Y., Ye, W., Yu, L., Liu, J., 2018. 3-Dehydroandrographolide protects against lipopolysaccharide-induced inflammation through the cholinergic anti-inflammatory pathway. Biochem Pharmacol 158, 305–317.
Lu, Z., Yang, H., Cao, H., Huo, C., Chen, Y., Liu, D., Xie, P., Zhou, H., Liu, J., Yu, L., 2020. Forsythoside a protects against lipopolysaccharide-induced acute lung injury through up-regulating microRNA-124. Clin Sci (Lond) 134, 2549–2563.
Luan, Z.G., Zhang, H., Yang, P.T., Ma, X.C., Zhang, C., Guo, R.X., 2010. HMGB1 activates nuclear factor-κB signaling by RAGE and increases the production of TNF-α in human umbilical vein endothelial cells. Immunobiology 215, 956–962.
Lv, J., Jia, Y., Li, J., Kuai, W., Li, Y., Guo, F., Xu, X., Zhao, Z., Lv, J., Li, Z., 2019. Gegen Qinlian decoction enhances the effect of PD-1 blockade in colorectal cancer with microsatellite stability by remodelling the gut microbiota and the tumour microenvironment. Cell Death Dis 10, 415.
Ma, N., Liu, X.W., Yang, Y.J., Li, J.Y., Mohamed, I., Liu, G.R., Zhang, J.Y., 2015. Preventive effect of aspirin eugenol ester on thrombosis in κ-Carrageenan-Induced rat tail thrombosis model. Plos One 10, e133125.
Mangan, M., Olhava, E.J., Roush, W.R., Seidel, H.M., Glick, G.D., Latz, E., 2018. Targeting the NLRP3 inflammasome in inflammatory diseases. Nat Rev Drug Discov 17, 588–606.
Manne, B.K., Münzer, P., Badolia, R., Walker-Allgaier, B., Campbell, R.A., Middleton, E., Weyrich, A.S., Kunapuli, S.P., Borst, O., Rondina, M.T., 2018. PDK1 governs thromboxane generation and thrombosis in platelets by regulating activation of Raf1 in the MAPK pathway. J Thromb Haemost 16, 1211–1225.
Paudel, Y.N., Khan, S.U., Othman, I., Shaikh, M.F., 2021. Naturally occurring HMGB1 inhibitor, glycyrrhizin, modulates chronic Seizures-Induced memory dysfunction in zebrafish model. Acs Chem Neurosci 12, 3288–3302.
Rad, F., Dabbagh, A., Dorgalaleh, A., Biswas, A., 2021. The relationship between inflammatory cytokines and coagulopathy in patients with COVID-19. J Clin Med 10.
Recabarren-Leiva, D., Burgos, C.F., Hernández, B., Garcïa-García, F.J., Castro, R.I., Guzman, L., Fuentes, E., Palomo, I., Alarcón, M., 2021. Effects of the age/rage axis in the platelet activation. Int J Biol Macromol 166, 1149–1161.
Satta, N., Kruithof, E.K., Fickentscher, C., Dunoyer-Geindre, S., Boehlen, F., Reber, G., Burger, D., de Moerloose, P., 2011. Toll-like receptor 2 mediates the activation of human monocytes and endothelial cells by antiphospholipid antibodies. Blood 117, 5523–5531.
Singh, B., Biswas, I., Bhagat, S., Surya, K.S., Khan, G.A., 2016. HMGB1 facilitates hypoxia-induced vWF upregulation through TLR2-MYD88-SP1 pathway. Eur J Immunol 46, 2388–2400.
Stark, K., Philippi, V., Stockhausen, S., Busse, J., Antonelli, A., Miller, M., Schubert, I., Hoseinpour, P., Chandraratne, S., von Brühl, M.L., Gaertner, F., Lorenz, M., Agresti, A., Coletti, R., Antoine, D.J., Heermann, R., Jung, K., Reese, S., Laitinen, I., Schwaiger, M., Walch, A., Sperandio, M., Nawroth, P.P., Reinhardt, C., Jäckel, S., Bianchi, M.E., Massberg, S., 2016. Disulfide HMGB1 derived from platelets coordinates venous thrombosis in mice. Blood 128, 2435–2449.
Totzeck, M., Mincu, R.I., Mrotzek, S., Schadendorf, D., Rassaf, T., 2018. Cardiovascular diseases in patients receiving small molecules with anti-vascular endothelial growth factor activity: A meta-analysis of approximately 29,000 cancer patients. Eur J Prev Cardiol 25, 482–494.
Varga, G., Lajkó, N., Ugocsai, M., Érces, D., Horváth, G., Tóth, G., Boros, M., Ghyczy, M., 2016. Reduced mucosal side-effects of acetylsalicylic acid after conjugation with tris-hydroxymethyl-aminomethane. Synthesis and biological evaluation of a new anti-inflammatory compound. Eur J Pharmacol 781, 181–189.
Vogel, S., Thein, S.L., 2018. Platelets at the crossroads of thrombosis, inflammation and haemolysis. Br J Haematol 180, 761–767.
Watanabe-Kusunoki, K., Nakazawa, D., Ishizu, A., Atsumi, T., 2020. Thrombomodulin as a physiological modulator of intravascular injury. Front Immunol 11, 575890.
Xu, Q., Bo, L., Hu, J., Geng, J., Chen, Y., Li, X., Chen, F., Song, J., 2018. High mobility group box 1 was associated with thrombosis in patients with atrial fibrillation. Medicine (Baltimore) 97, e132.
Yong, H.Y., Koh, M.S., Moon, A., 2009. The p38 MAPK inhibitors for the treatment of inflammatory diseases and cancer. Expert Opin Investig Drugs 18, 1893–1905.
Zhang, Q., Lenardo, M.J., Baltimore, D., 2017. 30 years of NF-κB: A blossoming of relevance to human pathobiology. Cell 168, 37–57.
Zhang, S., Liu, Y., Wang, X., Yang, L., Li, H., Wang, Y., Liu, M., Zhao, X., Xie, Y., Yang, Y., Zhang, S., Fan, Z., Dong, J., Yuan, Z., Ding, Z., Zhang, Y., Hu, L., 2020. SARS-CoV-2 binds platelet ACE2 to enhance thrombosis in COVID-19. J Hematol Oncol 13, 120.
Zhang, Y., Ma, X.J., Guo, C.Y., Wang, M.M., Kou, N., Qu, H., Mao, H.M., Shi, D.Z., 2016. Pretreatment with a combination of ligustrazine and berberine improves cardiac function in rats with coronary microembolization. Acta Pharmacol Sin 37, 463–472.